J|A|C|S
ARTICLES

Synthesis and Electronic Structure of Cationic, Neutral, and Anionic Bis(imino)pyridine Iron Alkyl Complexes: Evaluation of Redox Activity in Single-Component Ethylene Polymerization Catalysts

Aaron M. Tondreau,[†] Carsten Milsmann,[‡] Andrew D. Patrick,[†] Helen M. Hoyt,[†]
Emil Lobkovsky,[†] Karl Wieghardt,[‡] and Paul J. Chirik*,[†]

*Baker Laboratory, Department of Chemistry and Chemical Biology, Cornell University,
Ithaca, New York 14853, and Max-Planck Institute for Bioinorganic Chemistry,
Stiftstrasse 34-36, D-45470 Mülheim an der Ruhr, Germany*

Received August 4, 2010; E-mail: pc92@cornell.edu

Abstract: A family of cationic, neutral, and anionic bis(imino)pyridine iron alkyl complexes has been prepared, and their electronic and molecular structures have been established by a combination of X-ray diffraction, Mössbauer spectroscopy, magnetochemistry, and open-shell density functional theory. For the cationic complexes, $[(^{iPr}PDI)Fe-R][BPh_4]$ ($^{iPr}PDI = 2,6\text{-}(2,6\text{-}^{i}Pr_2\text{-}C_6H_3N=CMe)_2C_5H_3N$; $R = CH_2SiMe_3$, CH_2CMe_3, or CH_3), which are known single-component ethylene polymerization catalysts, the data establish high spin ferrous compounds ($S_{Fe} = 2$) with neutral, redox-innocent bis(imino)pyridine chelates. One-electron reduction to the corresponding neutral alkyls, $(^{iPr}PDI)Fe(CH_2SiMe_3)$ or $(^{iPr}PDI)Fe(CH_2CMe_3)$, is chelate-based, resulting in a bis(imino)pyridine radical anion ($S_{PDI} = \frac{1}{2}$) antiferromagnetically coupled to a high spin ferrous ion ($S_{Fe} = 2$). The neutral neopentyl derivative was reduced by an additional electron and furnished the corresponding anion, $[Li(Et_2O)_3][(^{iPr}PDI)Fe(CH_2CMe_3)N_2]$, with concomitant coordination of dinitrogen. The experimental and computational data establish that this $S = 0$ compound is best described as a low spin ferrous compound ($S_{Fe} = 0$) with a closed-shell singlet bis(imino)pyridine dianion ($S_{PDI} = 0$), demonstrating that the reduction is ligand-based. The change in field strength of the bis(imino)pyridine coupled with the placement of the alkyl ligand into the apical position of the molecule induced a spin state change at the iron center from high to low spin. The relevance of the compounds and their electronic structures to olefin polymerization catalysis is also presented.

Introduction

Aryl-substituted bis(imino)pyridine iron and cobalt dichloride complexes, $(^{Ar}PDI)MCl_2$ (M = Fe, Co), when activated with methylaluminoxane (MAO), exhibit high activities for ethylene and α-olefin oligomerization and polymerization.[1] Since the initial, independent reports in 1998 by Brookhart[2] and Gibson,[3,4] many studies have focused on alteration of the modular bis(imino)pyridine ligand framework[5,6] to establish structure−reactivity relationships. For the iron compounds, precatalysts bearing two large 2,6-substituents on the aryl ring are known to produce linear polyethylene, whereas those with only a single *ortho* aryl substituent are selective for α-olefin production with nearly ideal Schultz−Flory distributions.[7−9]

Despite a fairly mature understanding of how catalyst structure influences the type of oligomer or polymer produced, the mechanism of olefin polymerization and the nature of the active species formed upon treatment of $(^{Ar}PDI)FeCl_2$ with MAO remain controversial. Talsi and co-workers have conducted a series of extensive ^1H and ^2H NMR spectroscopic investigations to identify catalytic intermediates following addition of MAO, $AlMe_3$, $AlMe_3/B(C_6F_5)_3$, $AlMe_3/[Ph_3C][B(C_6F_5)_4]$, or other trialkylaluminum compounds to $(^{iPr}PDI)FeCl_2$.[10−12] Kinetic studies have identified that two distinct iron(II) species are

† Cornell University.
‡ Max-Planck Institute for Bioinorganic Chemistry.
(1) Bianchini, C.; Giambastiani, G.; Rios, I. G.; Mantovani, G.; Meli, A.; Segarra, A. M. *Coord. Chem. Rev.* **2006**, *250*, 1391.
(2) (a) Small, B. M.; Brookhart, M. *J. Am. Chem. Soc.* **1998**, *120*, 7143. (b) Small, B. L.; Brookhart, M.; Bennett, A. M. A. *J. Am. Chem. Soc.* **1998**, *120*, 4049.
(3) Britovsek, G. J. P.; Gibson, V. C.; Kimberley, B. S.; Maddox, S. J.; Solan, G. A.; White, A. J. P.; Williams, D. J. *Chem. Commun.* **1998**, 849.
(4) Britovsek, G. J. P.; Bruce, M.; Gibson, V. C.; Kimberely, B. S.; Maddox, P. J.; Mastroianni, S.; McTavish, S. J.; Redshaw, C.; Solan, G. A.; Strömberg, S.; White, A. J. P.; Williams, D. J. *J. Am. Chem. Soc.* **1999**, *121*, 8728.
(5) Gibson, V C.; Redshaw, C.; Solan, G. A. *Chem. Rev.* **2007**, *107*, 1745.
(6) Matsugi, T.; Fujita, T. *Chem. Soc. Rev.* **2008**, *37*, 1264.

(7) Britovsek, G. J. P.; Mastroianni, S.; Solan, G. A.; Baugh, C.; Redshaw, C.; Gibson, V. C.; White, A. J. P.; Williams, D. J.; Elsegood, M. R. J. *Chem.−Eur. J.* **2000**, *6*, 2221.
(8) Ionkin, A. S.; Marshall, W. J.; Adelman, D. J.; Fones, B. B.; Fish, B. M.; Schiffhauer, M. F. *Organometallics* **2008**, *27*, 1147.
(9) Ionkin, A. S.; Marshall, W. J.; Adelman, D. J.; Fones, B. B.; Fish, B. M.; Schiffhauer, M. F.; Soper, P. D.; Waterland, R. L.; Spence, R. E.; Xie, T. Y. *J. Polym. Sci., Part A* **2008**, *46*, 585.
(10) Talsi, E. P.; Babushkin, D. E.; Semikolenova, N. V.; Zudin, V. N.; Panchenko, V. N.; Zakharov, V. A. *Macromol. Chem. Phys.* **2001**, *202*, 2046.
(11) Bryliakov, K. P.; Semikolvenova, N. V.; Zudin, V. N.; Zakharov, V. A.; Talsi, E. P. *Chem. Commun.* **2004**, *5*, 45.
(12) Bryliakov, K. P.; Semikolvenova, N. V.; Zudin, V. N.; Zakharov, V. A.; Talsi, E. P. *Organometallics* **2004**, *23*, 5375.

Scheme 1. Synthetic Routes to Bis(imino)pyridine Iron Di- and Monoalkyl Complexes
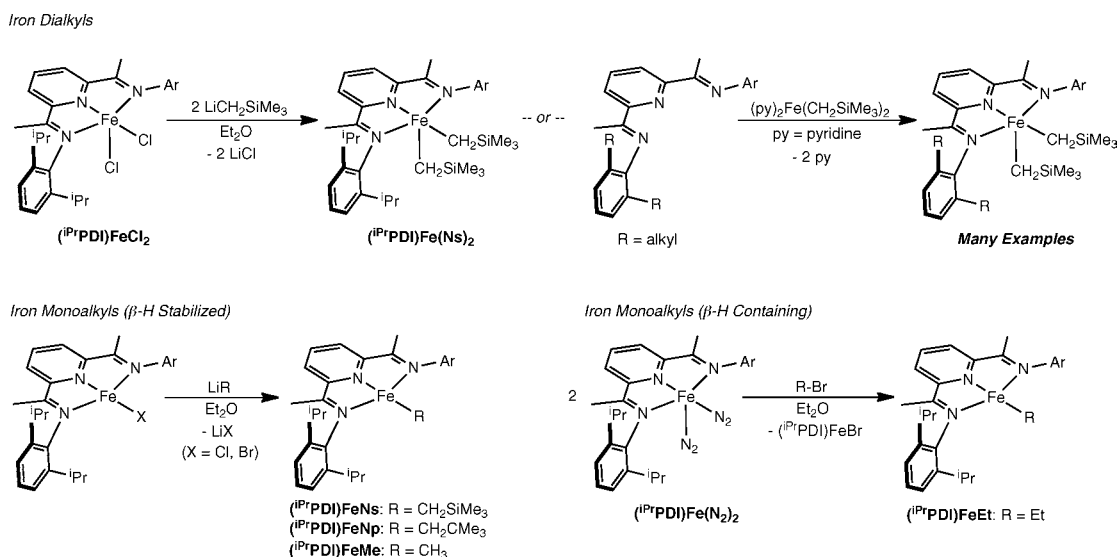

present during the polymerization that are respectively responsible for forming the low- and high-molecular weight polyethylene.[13-15] EPR and Mössbauer spectroscopic studies from Gibson and co-workers postulated formation of an iron(III) species upon activation with excess MAO,[16] and recent DFT studies suggest that this oxidation state is more active than the Fe(II) alternative.[17] Most recently, Bryliakov, Talsi, and co-workers studied the interaction of (^{iPr}PDI)FeCl$_2$ with MAO and aluminum trialkyls by NMR and EPR spectroscopies and identified [(^{iPr}PDI)Fe(μ-Me)$_2$AlMe$_2$], [(^{iPr}PDI)Fe(μ-^{i}Bu) (μ-X)Al(^{i}Bu)$_2$] (X = ^{i}Bu, Cl), and [(^{iPr}PDI)Fe(μ-Me)$_2$AlMe$_2$][MeMAO] after activation.[18]

Single-component olefin polymerization catalysts offer advantages for mechanistic studies, as characterization of the resting state, propagating species, and fundamental steps related to the initiation and termination of chain growth, in principle, is not complicated by the presence of a large excess of an ill-defined cocatalyst such as MAO. Such species may prove particularly insightful for bis(imino)pyridine iron-catalyzed olefin polymerization, given the ambiguities concerning iron oxidation state and bis(imino)pyridine participation in the electronic structure of the molecule and even chemical modification after treatment with an activator. Formally 14-electron, cationic metal alkyl species, [L$_n$M-R]$^+$X$^-$ (L$_n$ = supporting ligand(s); R = alkyl; X$^-$ = weakly coordinating, low-nucleophilicity anion), have proven to be effective single-component olefin polymerization catalysts in both group 4 transition metal chemistry[19-21] and group 10 metal chemistry.[22,23] These compounds are typically synthesized by treatment of the corresponding neutral metal dialkyl derivative, [L$_n$MR$_2$], with Brønsted[24,25] or Lewis acids[26] or an alkyl abstracting agent such as [Ph$_3$C][B(C$_6$F$_5$)$_4$].[27]

Guided by these precedents, the analogous, formally 14-electron bis(imino)pyridine iron alkyl cations, [(^{Ar}PDI)Fe-R]$^+$, have been long-standing targets for single-component iron polymerization catalysts.[28] Although successful for cobalt,[29-31] mono- and dialkyl complexes of bis(imino)pyridine iron remained elusive until 2005, when several groups independently

reported methods for their preparation.[32] Our laboratory reported direct alkylation of (^{iPr}PDI)FeCl$_2$ with LiCH$_2$SiMe$_3$ to yield (^{iPr}PDI)Fe(CH$_2$SiMe$_3$)$_2$, following recrystallization (Scheme 1).[33] Shortly thereafter, Gambarotta and co-workers reported that

(13) Barabanov, A. A.; Zakharov, V. A.; Semikolvenova, N. V.; Echevskaja, L. G.; Matsko, M. A. *Macromol. Chem. Phys.* **2005**, *206*, 2292.

(14) Barabanov, A. A.; Bukatov, G. D.; Zakharov, V. A.; Semikolvenova, N. V.; Mikenas, T. B.; Echevskaja, L. G.; Matsko, M. A. *Macromol. Chem. Phys.* **2005**, *207*, 1368.

(15) Kissin, Y. V.; Qian, C.; Xie, G.; Chen, Y. *J. Polym. Sci., Part A: Polym. Chem.* **2006**, *44*, 6159.

(16) Britovsek, G. J. P.; Clentsmith, G. K. B.; Gibson, V. C.; Goodgame, D. M. L.; McTavish, S. J.; Pankhurst, Q. A. *Catal. Commun.* **2002**, *3*, 207.

(17) Cruz, V. L.; Ramos, J.; Martinez-Salazar, J.; Gutierrez-Oliva, S.; Toro-Labbe, A. *Organometallics* **2009**, *28*, 5889.

(18) Bryliakov, K. P.; Talsi, E. P.; Semikolvenova, N. V.; Zakharov, V. A. *Organometallics* **2009**, *28*, 3225.

(19) (a) Mohring, P. C.; Coville, N. J. *Coord. Chem. Rev.* **2006**, *250*, 18. (b) Coates, G. W. *Chem. Rev.* **2000**, *100*, 1223. (c) Resconi, L.; Cavallo, L.; Fait, A.; Piemontesi, F. *Chem. Rev.* **2000**, *100*, 1253. (d) Ewen, J. A. *Sci. Am.* **1997**, *276*, 86.

(20) Jordan, R. F. *Adv. Organomet. Chem.* **1991**, *32*, 325.

(21) Erker, G. *Acc. Chem. Res.* **2001**, *34*, 309.

(22) (a) Speiser, F.; Braunstein, P.; Saussine, W. *Acc. Chem. Res.* **2005**, *38*, 784. (b) Zhang, W.; Zhang, W. J.; Sun, W. H. *Prog. Chem.* **2005**, *17*, 310. (c) Gibson, V. C.; Spitzmesser, S. K. *Chem. Rev.* **2003**, *103*, 283. (d) Ittel, S. D.; Johnson, L. K.; Brookhart, M. *Chem. Rev.* **2000**, *100*, 1169.

(23) Macchioni, A. *Chem. Rev.* **2005**, *105*, 2039.

(24) Brookhart, M.; Grant, B.; Volpe, A. F., Jr. *Organometallics* **1992**, *11*, 3920.

(25) Chen, E. Y. X.; Marks, T. J. *Chem. Rev.* **2000**, *100*, 1391.

(26) Yang, X. M.; Stern, C. L.; Marks, T. J. *J. Am. Chem. Soc.* **1994**, *116*, 10015.

(27) Chien, J. C. W.; Tsai, W.-M.; Rausch, M. D. *J. Am. Chem. Soc.* **1991**, *113*, 8570.

(28) Britovsek, G. J. P.; Gibson, V. C.; Spitzmesser, S. K.; Tellman, K. P.; White, A. J. P.; Williams, D. *J. Chem. Soc., Dalton Trans.* **2002**, *3*, 207.

(29) Kooistra, T. M.; Knijnenburg, Q.; Smits, J. M. M.; Horton, A. D.; Budzelaar, P. H. M.; Gal, A. W. *Angew. Chem., Int. Ed.* **2001**, *40*, 4719.

(30) Gibson, V. C.; Tellmann, K. P.; Humphries, M. J.; Wass, D. F. *Chem. Commun.* **2002**, 2316.

(31) Tellmann, K. P.; Humphries, M. J.; Rzepa, H. S.; Gibson, V. C. *Organometallics* **2004**, *23*, 5503.

(32) Trovitch, R. J.; Lobkovsky, E.; Chirik, P. J. *J. Am. Chem. Soc.* **2008**, *130*, 11631.

(33) Bouwkamp, M. W.; Bart, S. C.; Hawrelak, E. J.; Trovitch, R. J.; Lobkovsky, E.; Chirik, P. J. *Chem. Commun.* **2005**, 3406.

Scheme 2. Cationic Bis(imino)pyridine Iron Alkyl Complexes as Single-Component Ethylene Polymerization Catalysts
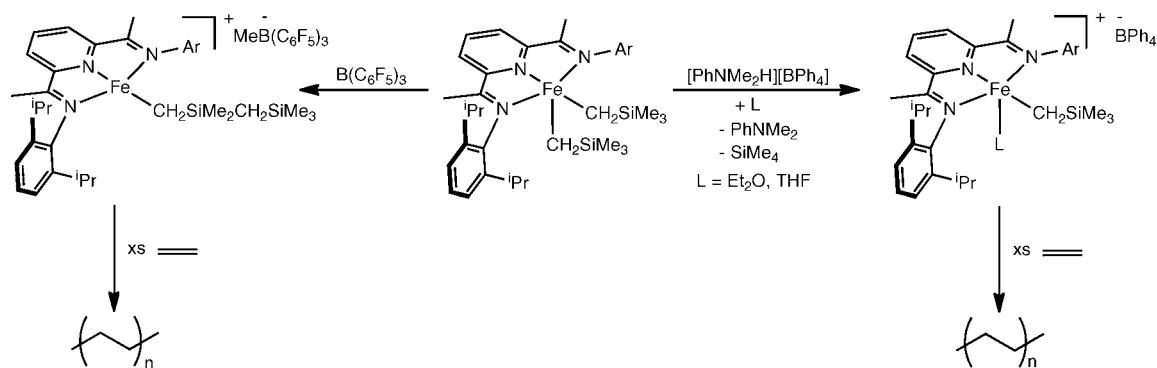
chelate alkylation can be competitive with iron alkylation under certain experimental conditions.[34] Cámpora and co-workers described an alternative route to $(^{Ar}PDI)Fe(CH_2SiMe_3)_2$ compounds where the free chelate is added to independently or in situ prepared $(pyridine)_2Fe(CH_2SiMe_3)_2$ (Scheme 1).[35] This method has proven versatile for the introduction of various bis(imino)pyridine chelates[36] and enantiopure pyridine bis(oxazoline) ligands.[37] However, simply substituting $(pyridine)_2$-$Fe(CH_2SiMe_3)_2$ with the neopentyl analogue resulted in competing alkyl migration and iron alkyl homolysis, suggesting this route is likely limited to β-silyl-substituted alkyls.[36]

Bis(imino)pyridine iron monoalkyl complexes have also been reported and have been prepared by direct alkylation of the corresponding monohalide precursor.[33,36] In this manner, several β-hydrogen-stabilized iron alkyl complexes, such as (^{iPr}PDI)-$FeCH_3$, $(^{iPr}PDI)FeCH_2SiMe_3$, and $(^{iPr}PDI)FeCH_2CMe_3$, have been synthesized.[33,36] A route to kinetically unstable β-hydrogen-containing neutral iron alkyls such as $(^{iPr}PDI)FeCH_2CH_3$ has also been reported by our laboratory, involving treatment of the iron bis(dinitrogen) compound, $(^{iPr}PDI)Fe(N_2)_2$,[38] with the appropriate alkyl bromide.[39] This method unfortunately yields an equimolar mixture of the desired monoalkyl complex along with the iron monobromide compound, $(^{iPr}PDI)FeBr$.

Synthesis of the long-sought-after bis(imino)pyridine iron alkyl cations has been accomplished by protonation of $(^{iPr}PDI)Fe(CH_2SiMe_3)_2$ with $[PhNMe_2H][BPh_4]$ (Scheme 2). Crystalline compounds were obtained upon addition of Et_2O and THF, and both $[(^{iPr}PDI)Fe(CH_2SiMe_3)L][BPh_4]$ (L = Et_2O, THF) have been structurally characterized.[40] Addition of the neutral borane, $B(C_6F_5)_3$, to $(^{iPr}PDI)Fe(CH_2SiMe_3)_2$ yielded the four-coordinate, base-free iron cation, $[(^{iPr}PDI)Fe(CH_2SiMe_2-CH_2SiMe_3)][MeB(C_6F_5)_3]$, arising from alkyl rearrangement following silicon methide abstraction.[40−42] Upon exposure to

ethylene, all three iron compounds serve as single-component polymerization catalysts and yield linear polyethylene terminated by olefin end groups arising from β-hydrogen elimination. Cationic iron alkyl complexes with bidentate α-diimine[43] and nonconjugated diimine[44] supporting ligands have also been prepared, although ethylene polymerization activity was minimal in both cases. In the latter example, Bouwkamp's laboratory was able to observe, for the first time, reversible ethylene coordination to an iron alkyl cation. Gambarotta and co-workers also synthesized and isolated the *anionic* bis(imino)pyridine iron methyl complex, $[Li(THF)_4][(^{iPr}PDI)FeMe]$, and demonstrated its activity in ethylene polymerization upon treatment with excess MAO.[45]

Why are aryl-substituted bis(imino)pyridines such an effective ligand class in olefin polymerization[46] and other applications[47,48] of iron catalysis? The ease of synthesis, air-stability, and ability to rapidly prepare libraries of ligands are all practical advantages of bis(imino)pyridines that have likely increased their popularity. Bis(imino)pyridines are also well-established redox-active ligands and are known to promote reversible transfer of 1−3 electrons between the chelate and the transition metal.[49−54] This phenomenon gives rise to complexes whose formal oxidation state assignment can be deceiving but, more importantly, contributes to the catalytic performance of the complex, as the metal−ligand combination can smoothly adjust to the electronic requirements of a particular reaction surface and enable new chemistry.[55,56]

Key to the continued development of more productive and selective catalysts is elucidation of the mechanism of the

(34) Scott, J.; Gambarotta, S.; Korobkov, I.; Budzelaar, P. H. M. *J. Am. Chem. Soc.* **2006**, *128*, 9660.

(35) Campora, J.; Naz, A. M.; Palma, P.; Alvarez, E.; Reyes, M. L. *Organometallics* **2005**, *24*, 4878.

(36) Fernández, I.; Trovitch, R. J.; Lobkovsky, E.; Chirik, P. J. *Organometallics* **2008**, *27*, 109.

(37) Tondreau, A. M.; Darmon, J. M.; Wile, B. M.; Floyd, S. K.; Lobkovsky, E.; Chirik, P. J. *Organometallics* **2009**, *28*, 3928.

(38) Bart, S. C.; Lobkovsky, E.; Chirik, P. J. *J. Am. Chem. Soc.* **2004**, *126*, 13794.

(39) Trovitch, R. J.; Lobkovsky, E.; Chirik, P. J. *J. Am. Chem. Soc.* **2008**, *130*, 11631.

(40) Bouwkamp, M. W.; Lobkovsky, E.; Chirik, P. J. *J. Am. Chem. Soc.* **2005**, *127*, 9660.

(41) Cameron, T. M.; Gordon, J. C.; Michalczyk, R.; Scott, B. L. *Chem. Commun.* **2003**, 2282.

(42) Gielens, E. E. C. G.; Tiesnitsch, J. Y.; Hessen, B.; Teuben, J. H. *Organometallics* **1998**, *17*, 1652.

(43) Bart, S. C.; Hawrelak, E. J.; Schmisseur, A. K.; Lobkovsky, E.; Chirik, P. J. *Organometallics* **2004**, *23*, 237.

(44) Volbeda, J.; Meetsma, A.; Bouwkamp, M. W. *Organometallics* **2009**, *28*, 209.

(45) Scott, J.; Gambarotta, S.; Korobkov, I.; Budzelaar, P. H. M. *Organometallics* **2005**, *24*, 6298.

(46) Fayet, G.; Raybaud, P.; Toulhoat, H.; de Bruin, T. *J. Mol. Structure - Theochem* **2009**, *903*, 100.

(47) (a) Sylvester, K. T.; Chirik, P. J. *J. Am. Chem. Soc.* **2009**, *131*, 8772. (b) Bouwkamp, M. W.; Bowman, A. C.; Lobkovsky, E.; Chirik, P. J. *J. Am. Chem. Soc.* **2006**, *128*, 13340.

(48) Bauer, E. *Curr. Org. Chem.* **2008**, *12*, 1341.

(49) (a) Knijnenburg, Q.; Gambarotta, S.; Budzelaar, P. H. M. *Dalton Trans.* **2006**, 5442. (b) Bart, S. C.; Chlopek, K.; Bill, E.; Bouwkamp, M. W.; Lobkovsky, E.; Neese, F.; Wieghardt, K.; Chirik, P. J. *J. Am. Chem. Soc.* **2006**, *128*, 13901.

(50) Butin, K. P.; Beloglazkina, E. K.; Zyk, N. V. *Russ. Chem. Rev.* **2005**, *74*, 531.

(51) Kuwabara, I. H.; Comninos, F. C. M.; Pardini, V. L.; Viertler, H.; Toma, H. E. *Electrochim. Acta* **1994**, *39*, 2401.

(52) Toma, H. E.; Chavez-Gil, T. E. *Inorg. Chim. Acta* **1997**, *257*, 197.

(53) de Bruin, B.; Bill, E.; Bothe, E.; Weyermüller, T.; Wieghardt, K. *Inorg. Chem.* **2000**, *39*, 2936.

(54) Budzelaar, P. H. M.; de Bruin, B.; Gal, A. W.; Wieghardt, K.; van Lenthe, J. H. *Inorg. Chem.* **2001**, *40*, 4649.

polymerization reaction and identification of the active species. For bis(imino)pyridine iron-catalyzed reactions, chelate redox activity presents an additional challenge for determining the oxidation state of the metal center and understanding fundamental transformations relevant to chain initiation, growth, and termination. Here we describe a new, general synthetic method for the preparation of base-free, cationic bis(imino)pyridine iron alkyl compounds and evaluate the electronic structure of single-component iron ethylene polymerization catalysts. In addition, the electronic structure and degree of bis(imino)pyridine chelate participation is determined for a series of cationic, neutral, and anionic iron alkyl compounds that differ by three oxidation states, where redox changes occur at the ligand, not the metal.

Results and Discussion

Synthesis of Bis(imino)pyridine Iron Alkyl Cations. Our laboratory previously communicated the synthesis of cationic bis(imino)pyridine iron alkyl complexes by protonation or alkyl abstraction from the corresponding dialkyl precursor.[40,44] As documented previously,[33,35,36] only β-silyl-substituted bis(imino)pyridine iron dialkyl complexes, e.g., $(^{iPr}PDI)Fe(CH_2SiMe_3)_2$, are currently synthetically accessible. For example, pyridine displacement from either $(pyridine)_2Fe(CH_2CMe_3)_2$ or $(pyridine)_2$-$Fe(CH_2CMe_3)(CH_2SiMe_3)$ by addition of free bis(imino)pyridine ligand resulted in ejection of the neopentyl group and formation of iron monoalkyl complexes.[36] To prepare more polymerization relevant, pure hydrocarbyl-containing bis(imino)pyridine iron alkyl cations, new synthetic routes are necessary.

Four-coordinate, neutral bis(imino)pyridine iron alkyls that are stabilized with respect to β-hydrogen elimination are synthetically accessible by straightforward salt metathesis of the corresponding iron chloride or bromide complex with the appropriate alkyl lithium reagent.[33,36] This route offers an attractive entry into the desired alkyl cation chemistry via one-electron oxidation. Treatment of a benzene solution of $(^{iPr}PDI)FeCH_2CMe_3$ with $[(\eta^5\text{-}C_5H_5)_2Fe][BPh_4]$ resulted in precipitation of a light red powder, identified as the base-free bis(imino)pyridine iron neopentyl cation, $[(^{iPr}PDI)FeCH_2\text{-}CMe_3][BPh_4]$ (eq 1). Exposure of this product to either Et_2O or THF furnished the corresponding ligand-stabilized cations, $[(^{iPr}PDI)Fe(CH_2CMe_3)L][BPh_4]$ (L = Et_2O, THF), as light purple solids. Generation of $[(^{iPr}PDI)FeCH_2CMe_3][BPh_4]$ in situ in benzene-d_6 allowed collection of ^1H NMR data. For many of the isolated alkyl cations, NMR spectra were obtained in C_6D_5F, and the data are reported in the Experimental Section and are consistent with $S = 2$ iron compounds.

(^{iPr}PDI)FeCH_2CMe_3: E = C
(^{iPr}PDI)FeCH_2SiMe_3: E = Si

[(^{iPr}PDI)Fe(CH_2CMe_3)][BPh_4]: E = C
[(^{iPr}PDI)Fe(CH_2SiMe_3)][BPh_4]: E = Si
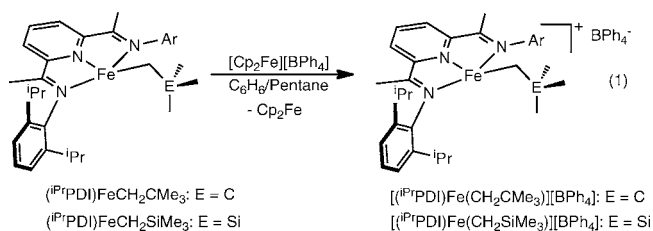
The successful synthesis of bis(imino)pyridine iron neopentyl cations from one-electron oxidation of the neutral alkyl precursor prompted exploration of the synthesis of the other bis(imino)pyridine iron alkyl complexes that were inaccessible from the previously reported iron dialkyl route. We previously reported in situ generation of $[(^{iPr}PDI)Fe(CH_2SiMe_3)][BPh_4]$ by treatment of the corresponding neutral bis(imino)pyridine iron dialkyl with $[PhNMe_2H][BPh_4]$ in a non-coordinating solvent such as toluene

or pentane, although isolation as a pure solid was not achieved.[40] One-electron oxidation of $(^{iPr}PDI)FeCH_2SiMe_3$ with $[(\eta^5\text{-}C_5H_5)_2Fe][BPh_4]$ in benzene followed by precipitation by addition of excess pentane furnished $[(^{iPr}PDI)FeCH_2SiMe_3]\text{-}[BPh_4]$ as a dull gray-red powder in 88% yield (eq 1). This material served as a precursor to the diethyl ether- and THF-stabilized cations, $[(^{iPr}PDI)Fe(CH_2SiMe_3)L][BPh_4]$ (L= Et_2O, THF),[40] by addition of a slight excess of the appropriate solvent.

The bis(imino)pyridine iron methyl cation, $[(^{iPr}PDI)Fe\text{-}(CH_3)]^+$, was also targeted due to its potential relevance to the active species obtained upon treatment of $(^{iPr}PDI)FeCl_2$ with MAO or $AlMe_3$ and to explore its role as a single-component olefin polymerization catalyst. As with the neopentyl and neosilyl compounds, oxidation of $(^{iPr}PDI)FeCH_3$ with $[(\eta^5\text{-}C_5H_5)_2Fe][BPh_4]$ in benzene followed by precipitation with pentane furnished a dull gray solid identified as $[(^{iPr}PDI)Fe\text{-}(CH_3)][BPh_4]$ (eq 2). Complete characterization and elucidation of the electronic structure of these molecules are presented in a later section of this article.
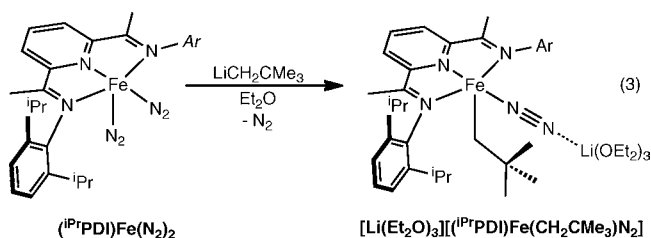

(^{iPr}PDI)FeCH_3

[(^{iPr}PDI)Fe(CH_3)][BPh_4]
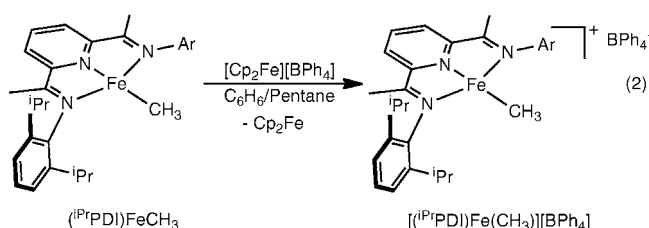
Synthesis of Bis(imino)pyridine Iron Alkyl Anions. The new route to various β-hydrogen-stabilized bis(imino)pyridine iron alkyl cations prompted exploration of the synthesis of related anionic alkyl complexes to complete a series of compounds that vary by three oxidation states that will allow systematic evaluation of chelate participation. Prior to this study, the only anionic bis(imino)pyridine iron alkyl complexes known were $[Li(THF)_4][(^{iPr}PDI)FeMe]$, reported by Gambarotta,[45] and the aryl anions, $[Li(Et_2O)_3][(^{iPr}PDI)Fe(C_6H_4\text{-}4\text{-}R)N_2]$ (R = H, Me), synthesized in our laboratory.[35] However, the electronic structure of these compounds and the redox activity of the bis(imino)pyridine chelate have not been determined.

Because both neutral and cationic bis(imino)pyridine neosilyl compounds, $[(^{iPr}PDI)FeCH_2SiMe_3]^{0/+}$, have been reported, the synthesis of the corresponding anion was targeted. Treatment of a diethyl ether solution of $(^{iPr}PDI)Fe(N_2)_2$ with 1 equiv of $LiCH_2SiMe_3$ resulted in a color change from green to purple, suggesting formation of the desired alkyl anion. However, attempts to isolate the product in the solid state by either recrystallization or solvent removal in vacuo resulted in isolation of the neutral bis(imino)pyridine iron alkyl compound, $(^{iPr}PDI)FeCH_2SiMe_3$.[36] Likewise, addition of 2 equiv of $LiCH_2SiMe_3$ to a diethyl ether solution of $(^{iPr}PDI)FeBr$ also yielded a purple reaction mixture, but again the neutral iron alkyl, $(^{iPr}PDI)FeCH_2SiMe_3$, was isolated. Attempts to intercept the anion by addition of 12-crown-4 to the purple solutions (generated by either method) were also unsuccessful.

(55) For representative examples of this concept in stoichiometric and catalytic reactions in early transition metal chemistry, see: (a) Zarkesh, R. A.; Ziller, J. W.; Heyduk, A. F. *Angew. Chem., Int. Ed.* **2008**, *47*, 4715. (b) Blackmore, K. J.; Lal, N.; Ziller, J. W.; Heyduk, A. F. *J. Am. Chem. Soc.* **2008**, *130*, 2728. (c) Stanciu, C.; Jones, M. E.; Fanwick, P. E.; Abu-Omar, M. M. *J. Am. Chem. Soc.* **2007**, *129*, 12400.

(56) Chirik, P. J.; Wieghardt, K. *Science* **2010**, *327*, 794.

Due to the complications associated with isolation of the iron neosilyl anion, attention was then devoted to the preparation of the corresponding neopentyl complex. Our laboratory has reported the synthesis of the neutral variant, $(^{iPr}PDI)FeCH_2CMe_3$, by straightforward salt metathesis of $(^{iPr}PDI)FeBr$ with $LiCH_2CMe_3$.[36] Treatment of a diethyl ether solution of $(^{iPr}PDI)Fe(N_2)_2$ with 1 equiv of $LiCH_2CMe_3$, followed by recrystallization at -35 °C, furnished a red-brown solid identified as $[Li(Et_2O)_3][(^{iPr}PDI)Fe(CH_2CMe_3)N_2]$ (eq 3). This compound was also prepared by addition of 2 equiv of $LiCH_2CMe_3$ to a diethyl ether solution of the bis(imino)pyridine iron bromide, $(^{iPr}PDI)FeBr$.[32] The crown ether derivative, $[Li(12\text{-}crown\text{-}4)][(^{iPr}PDI)Fe(CH_2CMe_3)(N_2)]$, was also synthesized by addition of 12-crown-4 to a diethyl ether solution of the initially generated anion. The diethyl ether solvate, $[Li(Et_2O)_3][(^{iPr}PDI)Fe(CH_2CMe_3)N_2]$, is an exceedingly reactive compound and undergoes decomposition in the solid state and in solution. For subsequent spectroscopic and crystallographic studies (vide infra), the compound was prepared and used immediately.

$$(^{iPr}PDI)Fe(N_2)_2 \xrightarrow[\substack{Et_2O \\ -N_2}]{LiCH_2CMe_3} [Li(Et_2O)_3][(^{iPr}PDI)Fe(CH_2CMe_3)N_2] \quad (3)$$

As was observed for $[Li(THF)_4][(^{iPr}PDI)FeMe]$[45] and $[Li(Et_2O)_3][(^{iPr}PDI)Fe(C_6H_4\text{-}4\text{-}Me)N_2]$,[36] $[Li(Et_2O)_3][(^{iPr}PDI)Fe(CH_2CMe_3)N_2]$ exhibits no observable or assignable ^1H NMR resonances in benzene-d_6 at 23 °C. This spectroscopic behavior contrasts with that of the neutral bis(imino)pyridine iron mono- and dialkyl complexes, where sharp, paramagnetically shifted resonances are observed and readily assigned.[33,35,32] Solid state magnetic measurements (magnetic susceptibility balance) on $[Li(solv)_n][(^{iPr}PDI)Fe(CH_2CMe_3)N_2]$ (solv = Et_2O, $n = 3$; 12-crown-4, $n = 1$) established diamagnetic molecules. Attempts were made to measure solution magnetic moments by Evans's method; however, the extreme sensitivity of the anions prohibited acquisition of reliable data. Monitoring the solution over short times in benzene-d_6 at 23 °C often revealed formation of free bis(imino)pyridine ligand as well as the corresponding neutral iron alkyl compound arising from oxidation of the anion. We note that these compounds were handled under the most stringent of air- and moisture-free conditions when the decomposition and oxidation processes were observed. Accordingly, the origin of the NMR-silent behavior is not currently understood.

Routine characterization of the bis(imino)pyridine iron neopentyl anions was accomplished by infrared spectroscopy, X-ray diffraction (solv = Et_2O), Mössbauer spectroscopy, solid state magnetic measurements, combustion analysis, and degradation experiments. The details of these experiments will be presented in a later section. Addition of excess water furnished free bis(imino)pyridine ligand, dinitrogen, and neopentane. Integration of the benzene-d_6 NMR spectrum following hydrolysis established 3 equiv of diethyl ether or 1 equiv of 12-crown-4 (per equivalent of free bis(imino)pyridine) for the different lithium solvates.

The terminal dinitrogen ligand in $[Li(solv)_n][(^{iPr}PDI)Fe(CH_2CMe_3)N_2]$ provides the most convenient spectroscopic handle for routine characterization. Dinitrogen coordination was

Table 1. Solid State (KBr) Infrared Stretching Frequencies of the N≡N Ligands in Bis(imino)pyridine Iron Alkyl and Aryl Anions[a]

| compound	ν (N≡N) (cm^{-1})
$[Li(OEt_2)_3][(^{iPr}PDI)Fe(CH_2CMe_3)N_2]$	1948
$[Li(Et_2O)_3][(^{iPr}PDI)Fe(C_6H_4\text{-}4\text{-}Me)(N_2)]$	1948
$[Li(12\text{-}crown\text{-}4)][(^{iPr}PDI)Fe(CH_2CMe_3)N_2]$	1996
$(^{iPr}PDI)FeN_2$	2046

[a] The neutral, four-coordinate dinitrogen complex, $(^{iPr}PDI)FeN_2$, is also included for comparison.

observed previously during the preparation and isolation of the related aryl anions, $[Li(Et_2O)_3][(^{iPr}PDI)Fe(C_6H_4\text{-}4\text{-}R)(N_2)]$ (R = H, Me).[35] The infrared stretching frequencies of the N≡N bands for each of these compounds recorded in the solid state (KBr) are presented in Table 1. The neutral bis(imino)pyridine iron mono(dinitrogen) compound, $(^{iPr}PDI)Fe(N_2)$, is also included for comparison.[38] As expected for the more reduced compounds, the dinitrogen stretching frequencies of the bis(imino)pyridine alkyl are significantly lower frequency than those of the neutral dinitrogen complex, $(^{iPr}PDI)Fe(N_2)$. For the same cation, both the iron tolyl and neopentyl anions contain N≡N bands at the same stretching frequency. As will be presented in a subsequent section, X-ray diffraction established that interaction of the $[Li(Et_2O)_3]^+$ cation with the terminal N_2 ligand is the same in both compounds. The most dramatic shift is observed for the 12-crown-4 compound and is likely a result of a different interaction of the cation with the anion rather than an indication of a gross change in electronic structure.

Crystallographic Characterization of Cationic and Anionic Bis(imino)pyridine Iron Alkyl Compounds. As is now well-established,[49] the metrical parameters of the bis(imino)pyridine ligand as determined from high-quality X-ray crystal structures are a reliable indicator of redox activity and hence key in the assignment of the oxidation states of both the ligand and the metal center. All metrical parameters for the bis(imino)pyridine iron compounds relevant to this study are reported in Tables 2 and 3. The solid state structure of the neutral bis(imino)pyridine iron neopentyl compound, $(^{Et}PDI)Fe(CH_2CMe_3)$, has been reported previously.[36] Note that the 2,6-aryl substituents on the bis(imino)pyridine ligand are ethyl groups, not isopropyl as in the compounds described in this study. However, this substitution is expected to have little impact on the overall electronic structure.

Single crystals of $[(^{iPr}PDI)Fe(CH_2CMe_3)][BPh_4]$ were obtained by cooling a concentrated fluorobenzene solution of the compound to -35 °C. A representation of the molecular structure is shown in Figure 1, and selected bond distances and angles are reported in Table 2. As was observed in the solid state structures of the neutral alkyl, $(^{Et}PDI)FeCH_2CMe_3$,[36] and in cationic iron neosilyls, $[(^{iPr}PDI)Fe(CH_2SiMe_3)L][BPh_4]$ (L = Et_2O, THF), and the related complex, $[(^{iPr}PDI)Fe(CH_2SiMe_2CH_2SiMe_3)][MeB(C_6F_5)_3]$,[40] the alkyl group in the cation is lifted out of the idealized square plane defined by the iron center and the bis(imino)pyridine chelate. There are no close contacts between the $[BPh_4]^-$ anion and the iron alkyl cation.

The bis(imino)pyridine iron methyl cation, $[(^{iPr}PDI)Fe(CH_3)][BPh_4]$, was also characterized by single-crystal X-ray diffraction, and a representation of the solid state structure is presented in Figure 2. As was observed with the neutral derivative, $(^{iPr}PDI)FeCH_3$, the geometry about iron is planar, with the sum of the angles around the metal equal to $359.99(27)$°. Because neopentyl and methyl would be expected to have nearly identical field strengths, the distortion in both the neutral and cationic
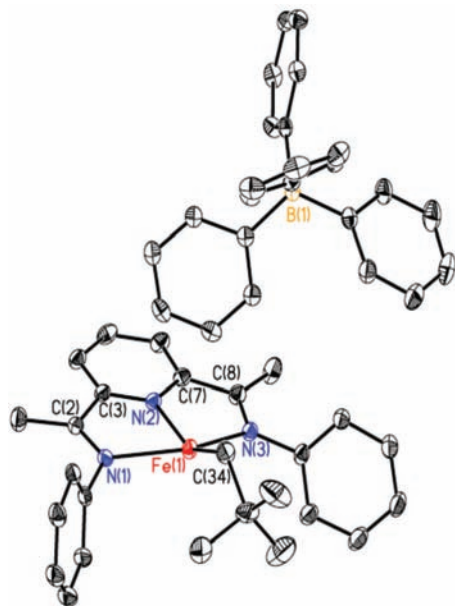
Figure 1. Representation of the solid state structure of [(iPrPDI)Fe-(CH₂CMe₃)][BPh₄] at 30% probability ellipsoids. Hydrogens and isopropyl aryl substituents are omitted for clarity.

Table 2. Metrical Parameters of Cationic, Neutral, and Anionic Bis(imino)pyridine Iron Neopentyl Complexes

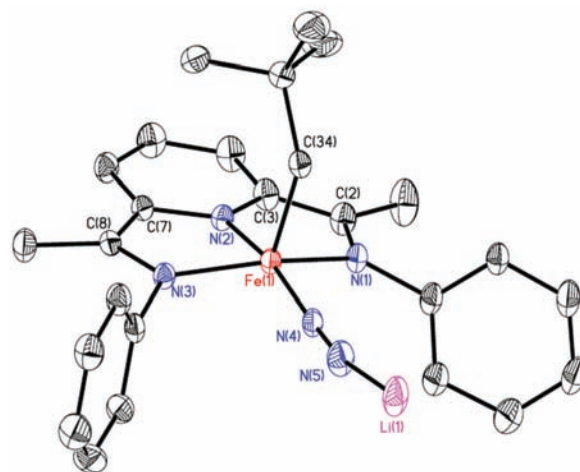|	[(iPrPDI)Fe(CH₂CMe₃)]-[BPh₄]	(EtPDI)Fe-(CH₂CMe₃)ᶜ	[(iPrPDI)Fe-(CH₂CMe₃)]⁻
Fe(1)−N(1)	2.213(2)	2.158(3)	1.931(2)
Fe(1)−N(2)	2.110(2)	1.986(3)	1.832(2)
Fe(1)−N(3)	2.242(2)	2.126(3)	1.919(2)
Fe(1)−N(4)			1.746(2)
Fe(1)−C(34)ᵃ	2.035(2)	2.036(4)	2.079(2)
N(1)−C(2)	1.284(2)	1.314(4)	1.361(3)
N(3)−C(8)	1.288(2)	1.329(4)	1.355(3)
N(2)−C(3)	1.333(2)	1.390(4)	1.386(3)
N(2)−C(7)	1.336(2)	1.366(4)	1.386(3)
C(2)−C(3)	1.490(3)	1.446(5)	1.394(3)
C(7)−C(8)	1.486(3)	1.428(5)	1.398(3)
N(4)−N(5)			1.138(3)
N(1)−Fe(1)−N(2)	73.14(6)	75.08(10)	80.17(8)
N(1)−Fe(1)−N(3)	142.87(6)	136.68(11)	154.90(8)
N(2)−Fe(1)−N(3)	72.83(6)	75.19(10)	79.85(8)
N(2)−Fe(1)−N(4)			167.76(9)
N(1)−Fe(1)−N(4)			98.45(9)
N(4)−Fe(1)−C(34)ᵇ			87.41(9)
N(2)−Fe(1)−C(34)ᵇ	151.61(8)	142.24(14)	104.82(9)

ᵃ Fe−C distance of the alkyl ligand. ᵇ The numbering scheme is different for the neutral and cationic alkyls. ᶜ Data from ref 36.

neopentyl (including neosilyl and related) complexes must be steric in origin. As with the base-free neopentyl cation, there are no close contacts between the [BPh₄]⁻ anion and the iron alkyl cation.

Single crystals of [Li(OEt₂)₃][(iPrPDI)Fe(CH₂CMe₃)(N₂)] were obtained from a concentrated diethyl ether solution cooled to −35 °C, and a representation of the solid state structure is presented in Figure 3. The crystals were large and fragile and did not diffract well. Each of the diethyl ether ligands on the [Li(Et₂O)₃]⁺ cation is severely disordered, and they were successfully modeled. The asymmetric unit also contained half of either a pentane or a diethyl ether molecule that was disordered and was removed by the SQUEEZE routine.
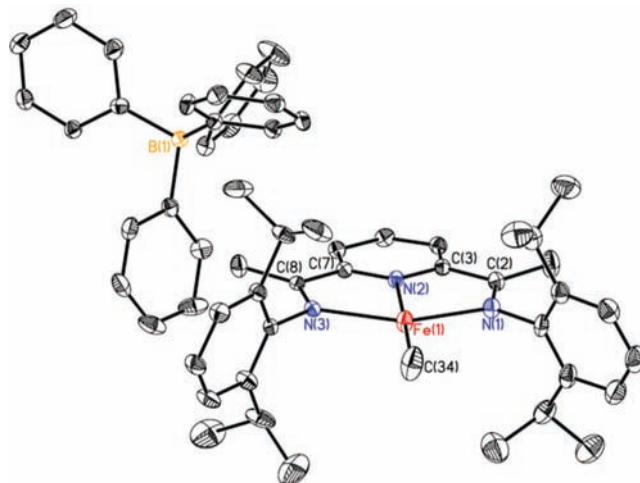
Figure 2. Representation of the solid state structure of [(iPrPDI)Fe-(CH₃)][BPh₄] at 30% probability ellipsoids. Hydrogens are omitted for clarity.

Figure 3. Representation of the solid state structure of [Li(OEt₂)₃]-[(iPrPDI)Fe(CH₂CMe₃)(N₂)] at 30% probability ellipsoids. Hydrogens, isopropyl aryl substituents, and the disordered diethyl ether ligands are omitted for clarity.

The overall molecular geometry of [(iPrPDI)Fe(CH₂CMe₃)-(N₂)]⁻ is best described as pseudo square pyramidal (keeping in mind the constraints of the chelate which distorts the basal plane away from an idealized square), with the alkyl ligand in the apical position and the dinitrogen molecule and the bis(imino)pyridine chelate defining the basal plane. This arrangement is likely preferred to maximize π-backbonding with the N₂ ligand and is corroborated by the relatively low N₂ stretching frequency observed by infrared spectroscopy. It is also possible that this arrangement is determined by the *trans* influence, where the strongest field ligand, the alkyl group, is apical and avoids the position *trans* to the *N*-pyridine, which is confined by the geometrical constraints of the ligand skeleton. The dinitrogen ligand is capped by the [Li(Et₂O)₃]⁺ cation, which also likely contributes to the reduced infrared stretching frequency. A similar overall molecular geometry was observed in the solid state structure of the previously characterized bis(imino)pyridine iron tolyl anion, [Li(Et₂O)₃][(iPrPDI)Fe(C₆H₄-4-Me)(N₂)].³⁶

The metrical parameters of the bis(imino)pyridine chelate in cationic, neutral, and anionic iron neopentyl derivatives are

Table 3. Metrical Parameters of Anionic, Neutral, and Cationic Bis(imino)pyridine Iron Methyl Complexes

	[Li(THF)$_4$]- [(^{iPr}PDI)Fe(CH$_3$)]$^{- \ a}$	(^{iPr}PDI)FeCH$_3$	[(^{iPr}PDI)Fe(CH$_3$)]- [BPh$_4$]
Fe(1)−N(1)	1.917(6)	1.968(5)	2.216(3)
Fe(1)−N(2)	1.849(6)	1.893(4)	2.117(3)
Fe(1)−N(3)	1.915(5)	1.952(5)	2.222(3)
Fe(1)−CH$_3$	2.013(9)	2.001(6)	2.006(4)
N(1)−C(2)	1.356(8)	1.337(7)	1.293(4)
N(3)−C(8)	1.377(9)	1.332(7)	1.286(4)
N(2)−C(3)	1.364(10)	1.349(7)	1.347(4)
N(2)−C(7)	1.387(10)	1.368(7)	1.333(4)
C(2)−C(3)	1.413(10)	1.432(8)	1.478(5)
C(7)−C(8)	1.406(10)	1.442(8)	1.493(5)
N(1)−Fe(1)−N(2)	80.6(3)	79.1(2)	73.29(11)
N(1)−Fe(1)−N(3)	178.9(4)	159.2(2)	146.26(11)
N(2)−Fe(1)−N(3)	80.0(3)	80.1(2)	72.97(11)

a Data from ref 45.

Table 4. Metrical Parameters of Anionic Bis(imino)pyridine Iron Alkyl Complexes and a Neutral (*N,N*-Dimethylamino)pyridine Compound for Comparison

	[(^{iPr}PDI)Fe- (CH$_2$CMe$_3$)N$_2$]$^-$	[(^{iPr}PDI)Fe- (C$_6$H$_4$-4-Me)N$_2$]$^{- \ a}$	(^{iPr}PDI)Fe(DMAP)^b
Fe(1)−N(1)	1.931(2)	1.927(2)	1.908(3)
Fe(1)−N(2)	1.832(2)	1.837(2)	1.821(3)
Fe(1)−N(3)	1.919(2)	1.927(2)	1.943(3)
Fe(1)−N(4)	1.746(2)	1.752(2)	1.979(3)
Fe(1)−C(34)	2.079(2)	2.005(2)	
N(1)−C(2)	1.361(3)	1.356(3)	1.350(5)
N(3)−C(8)	1.355(3)	1.354(3)	1.358(5)
N(2)−C(3)	1.386(3)	1.382(3)	1.390(5)
N(2)−C(7)	1.386(3)	1.380(3)	1.387(5)
C(2)−C(3)	1.394(3)	1.407(3)	1.414(5)
C(7)−C(8)	1.398(3)	1.402(4)	1.406(5)
N(1)−Fe(1)−N(2)	80.17(8)	79.89(8)	81.05(14)
N(1)−Fe(1)−N(3)	154.90(8)	154.89(8)	161.38(14)
N(2)−Fe(1)−N(3)	79.85(8)	79.55(8)	80.74(14)

a Data from ref 36. *b* Data from ref 38. DMAP = (*N,N*-dimethylamino)pyridine.

Table 5. Solid State Magnetic Moments of Bis(imino)pyridine Alkyl Compounds at 23 °C

compound	μ_{eff} (μ_B, 23 °C)
(^{iPr}PDI)Fe(CH$_2$CMe$_3$)	4.0^a
(^{iPr}PDI)Fe(CH$_2$SiMe$_3$)	3.8^a
[(^{iPr}PDI)Fe(CH$_2$CMe$_3$)][BPh$_4$]	4.8^b
[(^{iPr}PDI)Fe(CH$_2$CMe$_3$)(Et$_2$O)][BPh$_4$]	4.8^b
[(^{iPr}PDI)Fe(CH$_2$CMe$_3$)(THF)][BPh$_4$]	4.9^b
[(^{iPr}PDI)FeCH$_3$][BPh$_4$]	5.2^b

a Determined by the Evans method in benzene-d_6. Data from refs 33 and 36. *b* Determined by solid state magnetic susceptibility balance.

reported in Table 2 and indicate different ligand rather than metal oxidation states within the series of compounds. The cationic compound, [(^{iPr}PDI)Fe(CH$_2$CMe$_3$)][BPh$_4$], is the most straightforward to interpret, as the C$_{ipso}$−C$_{imine}$ and N$_{imine}$−C$_{imine}$ are relatively unperturbed from the free ligand[49] and are consistent with the neutral form of the bis(imino)pyridine. Thus, there is no redox activity in this compound, and the chelate is innocent. For the neutral compound, (^{Et}PDI)Fe(CH$_2$CMe$_3$), the chelate distances, as reported previously for compounds of this type,[36,49b] are consistent with one-electron reduction.

Selected metrical parameters for the iron methyl cation, [(^{iPr}PDI)Fe(CH$_3$)][BPh$_4$], are reported in Table 3. Also included in Table 3 are the distances for the neutral compound, (^{iPr}PDI)FeCH$_3$,[33] and Gambarotta's anionic variant, [Li(THF)$_4$]- [(^{iPr}PDI)FeCH$_3$].[45] As with [(^{iPr}PDI)Fe(CH$_2$CMe$_3$)][BPh$_4$], the metrical data for the chelate in [(^{iPr}PDI)Fe(CH$_3$)][BPh$_4$] are consistent with a neutral, redox-innocent bis(imino)pyridine. The elongated Fe−N$_{imine}$ bond distances of 2.216(3) and 2.222(3) Å are indicative of a high spin Fe(II) center.

The bis(imino)pyridine iron neopentyl and methyl anions, [(^{iPr}PDI)Fe(CH$_2$CMe$_3$)(N$_2$)]$^-$ [(^{iPr}PDI)Fe(CH$_3$)]$^-$, exhibit the largest chelate distortions in the two series and suggest the greatest degree of ligand reduction. To put these values in perspective, a second set of comparisons are made in Table 4. Included in Table 4 are the bond distances for [Li(OEt$_2$)$_3$][(^{iPr}PDI)-Fe(C$_6$H$_4$-4-Me)(N$_2$)][36] and (^{iPr}PDI)Fe(DMAP). The latter was included for comparison to an established intermediate spin ferrous compound with a two-electron-reduced bis(imino)-pyridine.[49b] For [Li(OEt$_2$)$_3$][(^{iPr}PDI)Fe(CH$_2$CMe$_3$)(N$_2$)], the N$_{imine}$−C$_{imine}$ distances of 1.361(3) and 1.355(3) Å are significantly elongated, while the C$_{imine}$−C$_{ipso}$ lengths of 1.394(3) and 1.398(3) Å are the most contracted of any bis(imino)pyridine iron compound crystallographically characterized to date. These values are similar to those reported for both [(^{iPr}PDI)FeMe]$^-$ and [(^{iPr}PDI)Fe(C$_6$H$_4$-4-Me)(N$_2$)]$^-$ and suggest either two-electron or possibly even three-electron[57] reduction of the chelate.

Magnetic Measurements. The magnetic ground state of each class of bis(imino)pyridine iron alkyl compound was also studied in the solid state by magnetic susceptibility balance, solution Evans method, and in some cases SQUID magnetometry. The alkyl anions, [Li(Et$_2$O)$_3$]][(^{iPr}PDI)Fe(CH$_2$CMe$_3$)N$_2$] and [Li(12-

crown-4)][(^{iPr}PDI)Fe(CH$_2$CMe$_3$)N$_2$], are diamagnetic and will not be discussed further. A summary of the magnetic moments determined at 23 °C for representative members of the series is reported in Table 5.

As reported previously,[33] the four-coordinate, neutral bis(imi-no)pyridine iron alkyls exhibit magnetic moments consistent with three unpaired electrons and $S = \frac{3}{2}$ ground states. The cationic alkyl complexes have magnetic moments indicative of $S = 2$ ground states, as described previously.[33,40] Variable-temperature SQUID magnetic data for the base-stabilized bis(imino)pyridine iron cation, [(^{iPr}PDI)Fe(CH$_2$CMe$_3$)(THF)]-[BPh$_4$], were also measured and are presented in Figure 4. Between 40 and 300 K, an essentially temperature-independent magnetic moment of 4.7 μ_B was measured, slightly lower than the expected spin-only value for four unpaired electrons but nevertheless consistent with an $S = 2$ ground state. Modeling the data established a *g* value of 1.906 and a *D* value of 6.6 cm^{-1}.

Mössbauer Spectroscopy. The cationic, neutral, and anionic bis(imino)pyridine iron alkyl complexes were also studied by zero-field ^{57}Fe Mössbauer spectroscopy. Representative spectra for the neopentyl series of compounds are presented in Figure 5, and parameters for all compounds described in this work are reported in Table 6. Also included in Table 6 are the iron the iron tolyl and methyl anions, [Li(Et$_2$O)$_3$][(^{iPr}PDI)Fe(C$_6$H$_4$-4-Me)N$_2$] and [Li(THF)$_4$][(^{iPr}PDI)FeMe], published by our labora-tory[36] and Gambarotta,[45] respectively.

Within the series of bis(imino)pyridine iron neopentyl compounds, the base-free cation, [(^{iPr}PDI)Fe(CH$_2$CMe$_3$)][BPh$_4$], exhibits the highest isomer shift, $\delta = 0.57$ mm s^{-1}, consistent

(57) Enright, D.; Gambarotta, S.; Yap, G. P. A.; Budzelaar, P. H. M. *Angew. Chem., Int. Ed.* **2002**, *41*, 3873.
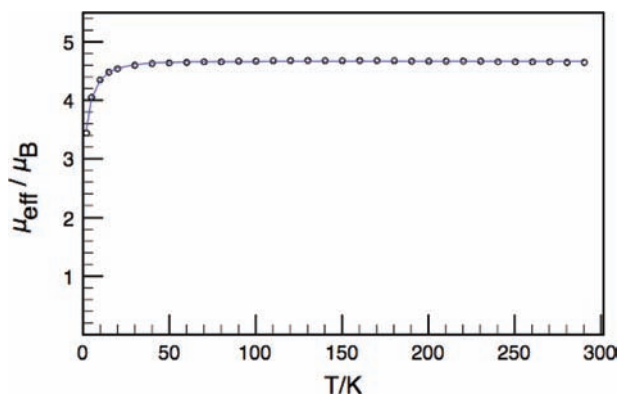
Figure 4. Temperature-dependent SQUID magnetization data (1 T) for [(^{iPr}PDI)Fe(CH$_2$CMe$_3$)THF][BPh$_4$] plotted as a function of magnetic moment (μ_{eff}) vs temperature (*T*). Data are corrected for underlying diamagnetism.

Table 6. Zero-Field ^{57}Fe Mössbauer Parameters Recorded at 80 K for Cationic, Neutral, and Anionic Bis(imino)pyridine Iron Alkyl and Dialkyl Compounds

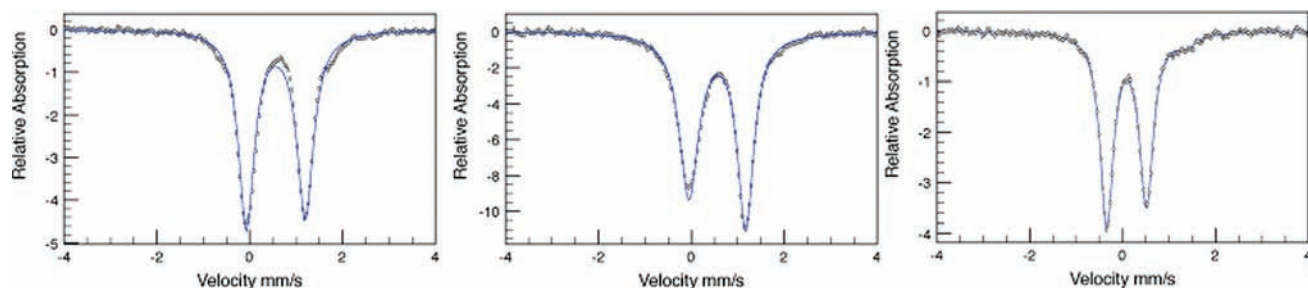| compound	δ (mm s^{-1})	ΔE_Q (mm s^{-1})
(^{iPr}PDI)Fe(CH$_2$CMe$_3$)	0.57	1.16
(^{Et}PDI)Fe(CH$_2$CMe$_3$)	0.56	1.13
(^{iPr}PDI)Fe(CH$_2$SiMe$_3$)	0.54	1.55
[(^{iPr}PDI)Fe(CH$_2$SiMe$_3$)][BPh$_4$]	0.64	1.35
[(^{iPr}PDI)Fe(CH$_2$SiMe$_3$)(Et$_2$O)][BPh$_4$]	0.88	2.20
[(^{iPr}PDI)Fe(CH$_2$SiMe$_3$)(THF)][BPh$_4$]	0.88	2.29
[(^{iPr}PDI)Fe(CH$_2$SiMe$_2$CH$_2$SiMe$_3$)][MeB(C$_6$F$_5$)$_3$]	0.61	1.37
[(^{iPr}PDI)Fe(CH$_2$CMe$_3$)][BPh$_4$]	0.57	1.30
[(^{iPr}PDI)Fe(CH$_2$CMe$_3$)(Et$_2$O)][BPh$_4$]	0.84	2.18
[(^{iPr}PDI)Fe(CH$_2$CMe$_3$)(THF)][BPh$_4$]	0.84	2.18
[(^{iPr}PDI)FeCH$_3$][BPh$_4$]	0.53	1.53
[(^{iPr}PDI)Fe(CH$_2$CMe$_3$)N$_2$]$^-$	0.06	0.86
[(^{iPr}PDI)Fe(CH$_3$)]$^-$	0.18	2.96
[(^{iPr}PDI)Fe(C$_6$H$_4$-4-Me)N$_2$]$^-$	0.02	0.93

with a high spin iron(II) center. Coordination of diethyl ether or THF results in a fairly significant increase in the isomer shift to 0.84 mm s^{-1}. This effect is a result of the overall increase in the metal−ligand bond distances as the coordination number increases from 4 to 5, resulting in an overall weaker ligand field and hence a decrease in charge density at the iron nucleus. Comparing the bond distances between the four-coordinate cation, [(^{iPr}PDI)Fe(CH$_2$SiMe$_2$CH$_2$SiMe$_3$)][MeB(C$_6$F$_5$)$_3$] versus the five-coordinate THF derivative, [(^{iPr}PDI)Fe(CH$_2$SiMe$_3$)-(THF)][BPh$_4$], the Fe(1)−C(34) distances increase from 2.011(6) to 2.034(3) Å, and the Fe(1)−N(1) and Fe−N(3) bond lengths increase from 2.217(4) to 2.286(2) Å and from 2.221(4) to 2.328(2) Å, respectively. The Fe(1)−N(2) distance, however, does not elongate and in fact slightly contracts from 2.121(4) to 2.089(2) Å. This may be due to the difference in the coplanarity of the iron and the bis(imino)pyridine between the two coordination environments. While addition of a coordinating solvent such as Et$_2$O or THF results in a significant change in isomer shift, reduction of the base-free neopentyl cation to the corresponding neutral compound, (^{iPr}PDI)Fe(CH$_2$CMe$_3$), has almost no effect, as identical isomer shifts were measured. This observation establishes little change in charge density at the iron nucleus and the same spectroscopic metal oxidation state between the two compounds.

The other bis(imino)pyridine iron alkyl cations exhibit similar isomer shifts, consistent with high spin iron(II) compounds. The base-free neosilyl cation, [(^{iPr}PDI)Fe(CH$_2$SiMe$_3$)][BPh$_4$], and the related rearranged alkyl compound, [(^{iPr}PDI)Fe(CH$_2$SiMe$_2$-CH$_2$SiMe$_3$][MeB(C$_6$F$_5$)$_3$], have isomer shifts of 0.64 and 0.61 mm s^{-1}, respectively. Likewise, for the base-free methyl cation, [(^{iPr}PDI)FeCH$_3$][BPh$_4$], a value of 0.53 mm s^{-1} was measured. As with the analogous neopentyl cations, addition of diethyl

ether or THF to [(^{iPr}PDI)Fe(CH$_2$SiMe$_3$)][BPh$_4$] results in a higher isomer shift of 0.88 mm s^{-1}, while formal one-electron reduction to the neutral compound, (^{iPr}PDI)Fe(CH$_2$SiMe$_3$), produced only a small shift to 0.54 mm s^{-1}, suggesting that the redox process is ligand rather than iron based and the Fe(II) oxidation state is maintained.

The Mössbauer isomer shifts of 0.06 and 0.02 mm s^{-1} for the bis(imino)pyridine tolyl and neopentyl anions, [Li(Et$_2$O)$_3$]-[(^{iPr}PDI)Fe(C$_6$H$_4$-4-Me)N$_2$] and [Li(Et$_2$O)$_3$][(^{iPr}PDI)Fe(CH$_2$-CMe$_3$)N$_2$], are significantly lower than those for the neutral alkyl complexes and indicate a significant change in charge density at the iron center. These values are lower than the reported isomer shift of 0.31 mm s^{-1} for (^{iPr}PDI)Fe(DMAP), an intermediate spin ($S_{Fe} = 1$) iron compound.[49b] The measured isomer shifts for the anionic complexes are comparable to the value of 0.03 mm s^{-1} reported for (^{iPr}PDI)Fe(CO)$_2$, a highly covalent molecule with contributions from both low spin Fe(II), closed-shell [PDI]$^{2-}$, and low spin Fe(0), d^8 canonical forms.[49b]
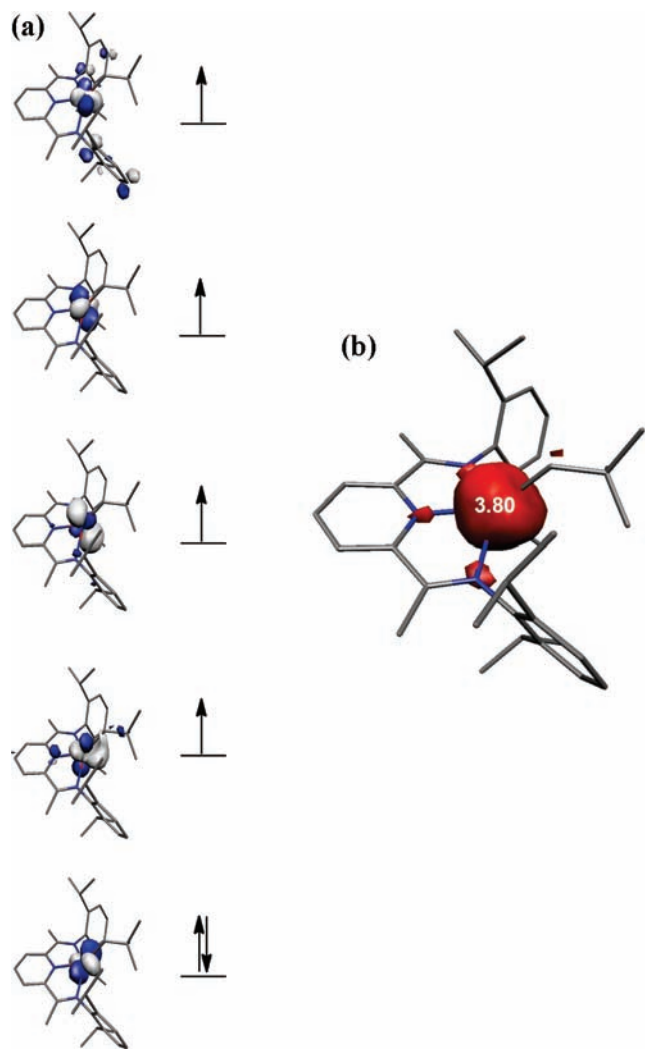
Computational Studies. DFT calculations using the B3LYP functional were also performed to gain additional insight into the electronic structure of the series of cationic, neutral, and anionic bis(imino)pyridine iron neopentyl compounds. For consistency within the computed series, all calculations were performed using the ^{iPr}PDI ligand.

For the base-free cation, [(^{iPr}PDI)Fe(CH$_2$CMe$_3$)]$^+$, a calculation assuming a simple quintet ground state successfully reproduced the metrical parameters determined by X-ray diffraction, including the deviation of the neopentyl group from idealized square planar geometry. The computed structure

Figure 5. Representative zero-field ^{57}Fe Mössbauer spectra of anionic (left), neutral (middle), and base-free cationic (right) bis(imino)pyridine iron neopentyl compounds.

Figure 6. (a) Qualitative molecular orbital diagram for $S = 2$ [(^{iPr}PDI)Fe(CH$_2$CMe$_3$)]$^+$ from a B3LYP DFT calculation. (b) Spin density plot obtained from a Mulliken population analysis (red, positive spin density; yellow, negative spin density).
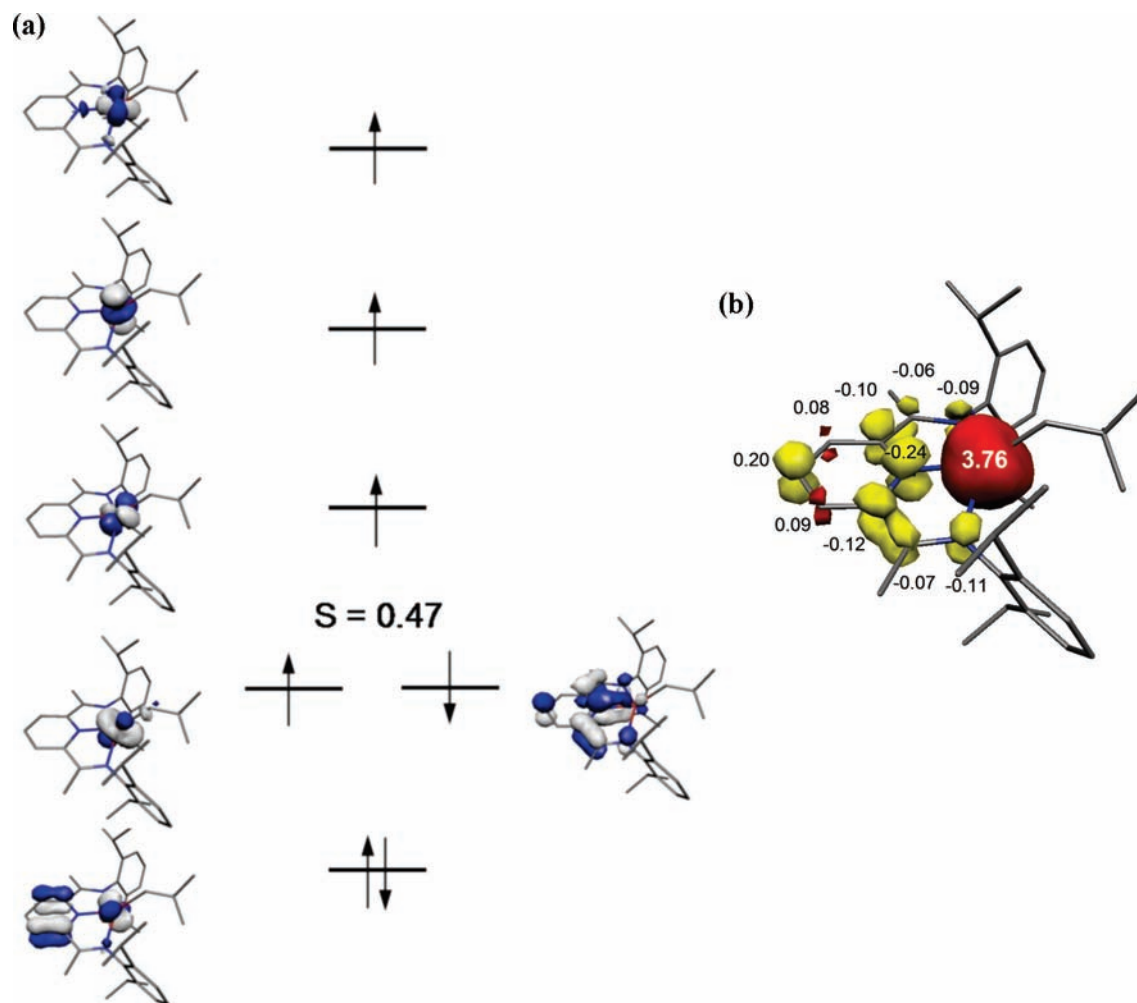
Table 7. Computed and Experimental Bond Distances (Å) and Angles (deg) for Cationic and Neutral Bis(imino)pyridine Iron Neopentyl Complexes

	[(^{iPr}PDI)Fe(CH$_2$CMe$_3$)]$^+$		(^{Et}PDI)Fe(CH$_2$CMe$_3$)		(^{iPr}PDI)Fe(CH$_2$CMe$_3$)
	expt	calcd	expt	calcd	calcd
Fe(1)−N(1)	2.213(2)	2.302	2.158(3)	2.286	2.334
Fe(1)−N(2)	2.210(2)	2.145	1.986(3)	2.033	2.040
Fe(1)−N(3)	2.242(2)	2.331	2.126(3)	2.226	2.281
Fe(1)−N(4)					
Fe(1)−C(34)	2.035(2)	2.034	2.036(4)	2.073	2.070
N(1)−C(2)	1.284(2)	1.286	1.314(4)	1.308	1.306
N(3)−C(8)	1.288(2)	1.285	1.329(4)	1.317	1.312
N(2)−C(3)	1.333(2)	1.340	1.390(4)	1.370	1.377
N(2)−C(7)	1.336(2)	1.340	1.366(4)	1.374	1.374
C(2)−C(3)	1.490(3)	1.497	1.446(5)	1.462	1.461
C(7)−C(8)	1.486(3)	1.498	1.428(5)	1.452	1.455
N(4)−N(5)					
N(1)−Fe(1)−N(2)	73.14(6)	72.68	75.08(10)	73.28	74.08
N(1)−Fe(1)−N(3)	142.87(6)	140.68	136.68(11)	137.79	140.85
N(2)−Fe(1)−N(3)	72.83(6)	72.21	75.19(10)	74.38	73.17
N(2)−Fe(1)−N(4)					
N(1)−Fe(1)−N(4)					
N(4)−Fe(1)−C(34)					
N(2)−Fe(1)−C(34)	151.61(8)	138.03	142.24(14)	138.88	145.25

lography for (^{Et}PDI)FeCH$_2$CMe$_3$. However, the imine−metal bond lengths are exceedingly overestimated by up to 0.17 Å. This is most likely due to the increased steric demand of the 2,6-diisopropyl aryl in the computational model rather than the ethyl substituents in the experimentally determined X-ray crystal structure. In fact, a geometry optimization of the 2,6-diethyl aryl-substituted compounds yielded significantly shorter imine−metal bonds, while the remaining structural parameters and electronic structure remained virtually unchanged (Table 7). Consistent with previous proposals,[36,49b] the computed electronic structure corresponds to a broken-symmetry (4,1) solution, obtained via spontaneous symmetry breaking during the unrestricted quartet calculation. The BS(m,n) descriptor refers to a broken symmetry state with m unpaired spin-up electrons on fragment 1 and n unpaired spin-down electrons essentially localized on fragment 2. A qualitative MO diagram and spin density plot are shown in Figure 7. Antiferromagnetic coupling between a singly occupied orbital of the high spin iron(II) ion and the bis(imino)pyridine radical, similar to the previously computed structure of (^{iPr}PDI)FeCl,[49b] accounts for the $S = {}^3/_2$ ground state. The computed ^{57}Fe Mössbauer parameters of $\delta = 0.57$ mm s^{-1} and $\Delta E_Q = +1.78$ mm s^{-1} are in excellent agreement with the experimentally determined values ($\delta = 0.57$ mm s^{-1}; $\Delta E_Q = |1.16$ mm s$^{-1}|$).

The final compound in the series, diamagnetic [(^{iPr}PDI)Fe-(CH$_2$CMe$_3$)N$_2$]$^-$, was also examined computationally. Initial studies were performed on the anionic component, [(^{iPr}PDI)Fe-(CH$_2$CMe$_3$)N$_2$]$^-$, without the lithium cation but with application of a COSMO solvation (THF) model to account for the negative charge. Two electronic structure descriptions were explored: a spin-restricted closed-shell structure and an open-shell BS(2,2) singlet alternative. Analysis of the computed electronic structures revealed that the closed-shell solution corresponds to a low spin Fe(II) ion coordinated by a closed-shell dianionic PDI^{2-} ligand with a doubly filled b$_2$ orbital, while the open-shell solution corresponds to an intermediate spin Fe(II) ion antiferromagnetically coupled to a triplet PDI^{2-} ligand. The energy difference between the two solutions was essentially indistinguishable, with the open shell being more stable by only 3.5

slightly overestimates the metal−ligand bond distances, a typical occurrence for the B3LYP functional.[58] The inclusion of solvent effects by applying the COSMO solvation model (THF) did not lead to significant changes of the geometric or electronic structure. A qualitative molecular orbital (MO) diagram and a spin density plot derived from these results (no COSMO solvation) are shown in Figure 6. This solution clearly establishes a high spin iron(II) ($S_{Fe} = 2$) configuration with a neutral, redox-innocent bis(imino)pyridine ligand, consistent with the metrical parameters of the chelate determined by X-ray diffraction. From this electronic structure description, computed ^{57}Fe Mössbauer parameters of $\delta = 0.58$ mm s^{-1} and $\Delta E_Q = -1.81$ mm s^{-1} were obtained that are in excellent agreement with the experimentally determined values ($\delta = 0.57$ mm s^{-1}; $\Delta E_Q = |1.30$ mm s$^{-1}|$).

The neutral bis(imino)pyridine iron neopentyl compound, (^{iPr}PDI)FeCH$_2$CMe$_3$, was calculated as a spin-unrestricted quartet on the basis of the experimentally determined $S = {}^3/_2$ ground state. Generally, the optimized geometry is in good agreement with the structural parameters obtained from X-ray crystal-

(58) Neese, F. *J. Biol. Inorg. Chem.* **2006**, *11*, 702.

Figure 7. (a) Qualitative molecular orbital diagram for $S = \frac{3}{2}$ (^{iPr}PDI)Fe(CH$_2$CMe$_3$) from a B3LYP DFT calculation. S represents the spatial overlap of the antiferromagnetically coupled magnetic orbitals. (b) Spin density plot obtained from a Mulliken population analysis (red, positive spin density; yellow, negative spin density).

kcal mol^{-1}. The structural parameters of both solutions are in reasonable agreement with the experimental values (see Table 8). The most significant differences were found for the Fe(1)−C(34) bond length, which is overestimated by almost 0.07 Å in the BS(2,2) approach but underestimated by only 0.01 Å in the closed-shell calculation. Similarly, the N(1)−C(2) and N(3)−C(8) distances are more accurately matched by the closed-shell singlet.

The ^{57}Fe Mössbauer parameters were calculated for both electronic structures to further substantiate the ground state of the molecule. Based on the broken-symmetry solution, values of $\delta = 0.29$ mm s^{-1} and $\Delta E_Q = +1.63$ mm s^{-1} were computed, which are in agreement with the data obtained for previously reported intermediate spin Fe(II) complexes with PDI ligands (e.g., (^{iPr}PDI)Fe(DMAP)^{49b} but disagree with the experimental parameters of $\delta = 0.06$ mm s^{-1} and $\Delta E_Q = |0.86$ mm s$^{-1}|$. By contrast, the closed-shell calculation reproduces the small quadrupole splitting, with a computed value of $\Delta E_Q = +1.09$ mm s^{-1}, but still overestimates the isomer shift significantly ($\delta = 0.25$ mm s^{-1}).

To investigate the influence of the terminal Li(Et$_2$O)$_3^+$ ion coordinated to the dinitrogen ligand, the molecule was calculated as [Li(Et$_2$O)$_3$][(^{iPr}PDI)Fe(CH$_2$CMe$_3$)N$_2$] without any truncations. Surprisingly, all attempts to obtain an open-shell singlet broken-symmetry solution for this compound failed and converged back

Table 8. Computed and Experimental Bond Distances (Å) and Angles (deg) for the Anionic Bis(imino)pyridine Iron Neopentyl Complex

|	[(^{iPr}PDI)FeN$_2$(CH$_2$CMe$_3$)]$^-$			[Li(Et$_2$O)$_3$][(^{iPr}PDI)FeN$_2$(CH$_2$CMe$_3$)]	
	expt	calcd BS(2,2)	calcd RKS	expt	calcd
Fe(1)−N(1)	1.931(2)	2.023	2.029	1.931(2)	2.043
Fe(1)−N(2)	1.832(2)	1.875	1.849	1.832(2)	1.851
Fe(1)−N(3)	1.919(2)	2.015	2.000	1.919(2)	2.033
Fe(1)−N(4)	1.746(2)	1.823	1.794	1.746(2)	1.756
Fe(1)−C(34)	2.079(2)	2.147	2.069	2.079(2)	2.076
N(1)−C(2)	1.361(3)	1.371	1.348	1.361(3)	1.353
N(3)−C(8)	1.355(3)	1.372	1.361	1.355(3)	1.349
N(2)−C(3)	1.386(3)	1.377	1.388	1.386(3)	1.390
N(2)−C(7)	1.386(3)	1.377	1.396	1.386(3)	1.387
C(2)−C(3)	1.394(3)	1.414	1.430	1.394(3)	1.421
C(7)−C(8)	1.398(3)	1.415	1.418	1.398(3)	1.425
N(4)−N(5)	1.138(3)	1.117	1.124	1.138(3)	1.137
N(1)−Fe(1)−N(2)	80.17(8)	80.17	79.79	80.17(8)	79.15
N(1)−Fe(1)−N(3)	154.90(8)	147.73	154.78	154.90(8)	154.11
N(2)−Fe(1)−N(3)	79.85(8)	80.03	79.93	79.85(8)	79.44
N(2)−Fe(1)−N(4)	167.76(9)	167.81	163.53	167.76(9)	165.44
N(1)−Fe(1)−N(4)	98.45(9)	96.69	97.58	98.45(9)	98.33
N(4)−Fe(1)−C(34)	87.41(9)	88.39	89.68	87.41(9)	88.79
N(2)−Fe(1)−C(34)	104.82(9)	103.80	106.79	104.82(9)	105.77

to the closed-shell solution. The structural parameters obtained from the geometry optimization of the full molecule are in excellent agreement with the experimental values. One notable exception is the significant overestimation of the iron−imine distances, which is slightly more pronounced than usually observed at the B3LYP level of theory. The calculated Mössbauer parameters of $\delta = 0.21$ mm s^{-1} and $\Delta E_Q = +1.12$ mm s^{-1} match the experimental values more closely than the values obtained for the truncated molecule (without the Li). However, the isomer shift is still notably overestimated, which is due to the elongated iron−imine bonds in the optimized geometry. Consequently, a spin-restricted closed-shell calculation on the crystallographic geometry yielded Mössbauer parameters of $\delta = 0.11$ mm s^{-1} and $\Delta E_Q = -0.96$ mm s^{-1}, in good agreement with experiment.

On the basis of these results, the electronic structure of [Li(Et$_2$O)$_3$][(^{iPr}PDI)Fe(CH$_2$CMe$_3$)N$_2$] is best described as a singlet with a low spin Fe(II) ion and a closed-shell ^{iPr}PDI^{2-} dianion. An important feature of this model is the strong covalent interaction of the axial neopentyl substituent with the d$_{z^2}$ orbital of the Fe center, which is most likely the reason for the spin state change from high spin to low spin upon reduction of the neutral compound to the anion. The corresponding MO diagram is shown in Figure 8. This description is in agreement with the structural data, which show very short metal−ligand bonds expected for low spin Fe(II) complexes and indicate two-electron ligand reduction.

Electronic Structure Summary. The combined synthetic, spectroscopic, and computational data obtained in this study establish a comprehensive view of the electronic structure of bis(imino)pyridine iron alkyl complexes that vary by three oxidation states. Importantly, these electronic structures are for single-component ethylene polymerization catalysts and resolve some of the controversy surrounding the nature of the active species upon activation of the dihalide complexes with MAO.

A summary of these findings is presented in Figure 9. The neutral four-coordinate iron monoalkyls, (^{iPr}PDI$^-$)Fe^{II}CH$_2$EMe$_3$ (E = C, Si), are used as the reference point. These compounds are best described as high spin ferrous derivatives antiferromagnetically coupled to a bis(imino)pyridine radical anion chelate. This configuration avoids formation of relatively rare Fe(I) alkyl species.[59] One-electron oxidation of the neutral iron monoalkyl compounds to the corresponding alkyl cations, [(^{iPr}PDI^0)Fe^{II}(CH$_2$EMe$_3$)]$^+$ (E = C, Si), is ligand-based, as both the experimental and computational data support high spin ferrous complexes with a redox-innocent neutral bis(imino)pyridine chelate. The analogous iron methyl cation, [(^{iPr}PDI^0)-Fe^{II}(Me)]$^+$, also has the same electronic structure description, despite the different geometry at the iron center. Given the single-component (i.e., no need for an activator) ethylene polymerization activity previously demonstrated for certain members of this series,[40] redox activity, at least in the initiating species, is *not* a prerequisite for polymerization activity. Studies with different metal−ligand complexes are currently under investigation to further support this claim.

The final member of the series is the monoalkyl anion, [(^{iPr}PDI^{2-})Fe^{II}(CH$_2$CMe$_3$)(N$_2$)]$^-$. Recall, the neosilyl variant proved inaccessible under conditions used to prepare the other examples reported in this work. The experimental and computational data establish that the electronic structure of [(^{iPr}PDI^{2-})Fe^{II}(CH$_2$CMe$_3$)(N$_2$)]$^-$ is best described as a low spin

(59) Holland, P. L. *Acc. Chem. Res.* **2008**, *41*, 905.
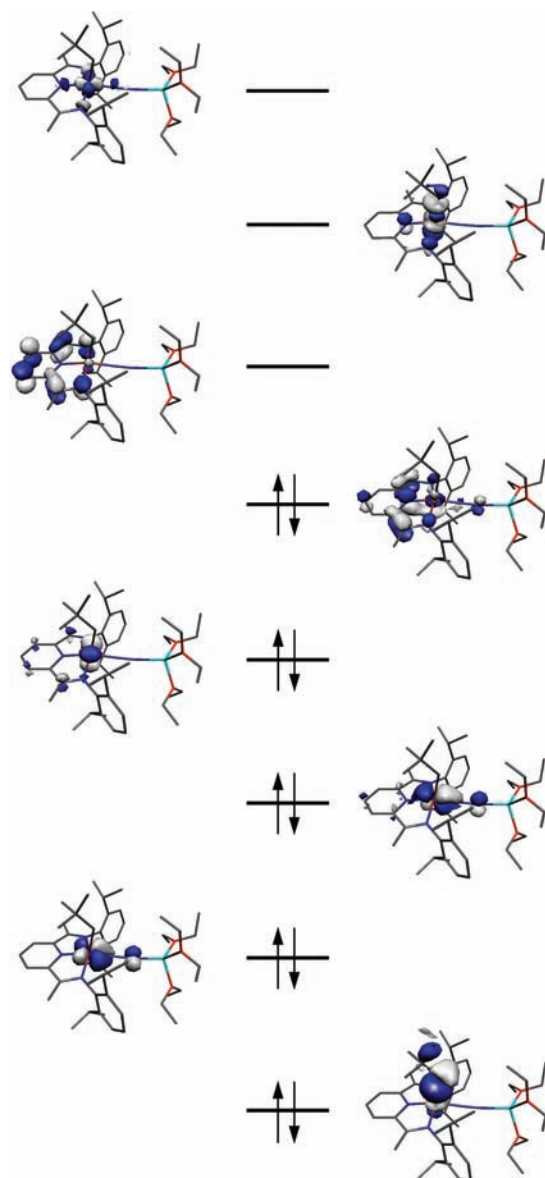
Figure 8. Qualitative molecular orbital diagram for $S = 0$ [(^{iPr}PDI)Fe(CH$_2$CMe$_3$)N$_2$]$^-$ from a B3LYP DFT calculation. The lowest energy orbital shown highlights the strong covalent interaction of the iron with the apical carbon donor of the alkyl.

ferrous compound ($S_{Fe} = 0$) with a closed-shell PDI^{2-} dianion. The low Mössbauer isomer shift and the extreme distortions to the chelate are consistent with this description. Notably, one-electron reduction of (^{iPr}PDI$^-$)Fe^{II}(CH$_2$CMe$_3$) is ligand-based and is also accompanied by a change in spin state (from high- to low spin ferrous) at the metal. As previous studies have shown, reduction of the bis(imino)pyridine ligand changes its field strength such that neutral and monoanionic forms are relatively weak field, while two-electron-reduced forms (either singlet or triplet) are stronger field.[49] Additionally, the shift of the strongly σ-donating neopentyl group to the apical position in the planar neutral complex to the axial position in the square pyramidal anion facilitates the change to the low spin configuration. For the neopentyl, tolyl, and phenyl derivatives prepared in our laboratory, the d^6 electron configuration of the low spin ferrous center is well established for π-backbonding and formation of dinitrogen complexes.
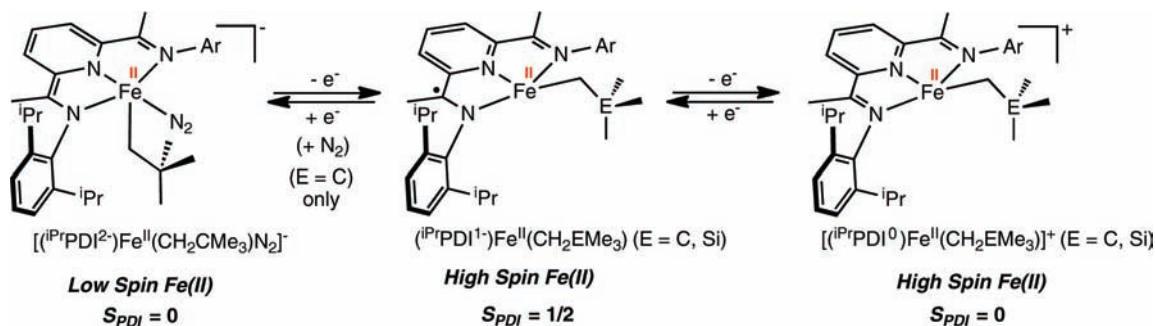
Figure 9. Electronic structure summary of cationic, neutral, and anionic bis(imino)pyridine iron alkyl and neutral iron dialkyl compounds.
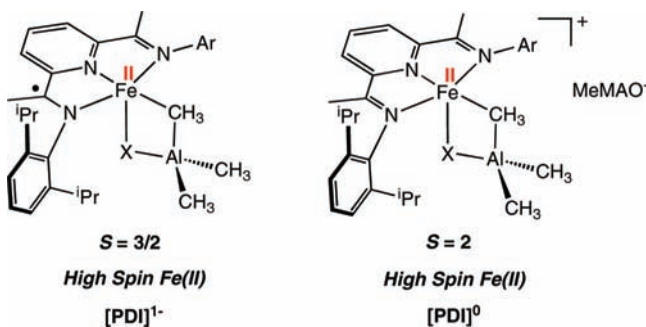

Figure 10. Proposed electronic structures for intermediates detected from treatment of (^{iPr}PDI)FeCl$_2$ with MAO and AlMe$_3$ (see ref 18).

The elucidation of the electronic structure of the cationic, neutral, and anionic bis(imino)pyridine iron monoalkyl complexes allows evaluation of the iron species proposed to form upon treatment of (^{iPr}PDI)FeCl$_2$ with MAO or AlMe$_3$ (Figure 10).[18] Recently, Bryliakov, Talsi, and co-workers reported observation of (^{iPr}PDI)Fe(μ-X)(μ-CH$_3$)Al(CH$_3$)$_2$ (X = Cl, CH$_3$) and [(^{iPr}PDI)Fe(μ-X)(μ-CH$_3$)Al(CH$_3$)$_2$]$^+$ by ^{1}H NMR and EPR spectroscopies.[18] The identity of X was determined by the relative ratio of MAO or AlMe$_3$ to the iron dihalide. For both the neutral and cationic complexes, these species were only observed in situ and were not isolated; hence, no crystallographic, magnetic, or Mössbauer data are available. However, on the basis of analogy to compounds prepared and studied in this work, electronic structures for both classes of compounds are proposed. The neutral compound, (^{iPr}PDI$^-$)Fe^{II}(μ-X)(μ-CH$_3$)Al(CH$_3$)$_2$, is best described as a ferrous compound with a bis(imino)pyridine radical anion. The cationic complex, [(^{iPr}PDI^0)-Fe^{II}(μ-X)(μ-CH$_3$)Al(CH$_3$)$_2$]$^+$, is likely a high spin ferrous compound (S_{Fe} = 2) with a redox-innocent, neutral bis(imino)pyridine chelate. Notably, our data suggest that treatment of (^{iPr}PDI)FeCl$_2$ with MAO or trialkylaluminums does not result in redox change at the iron center—all oxidation/reduction events occur at the bis(imino)pyridine ligand.

Concluding Remarks

Bis(imino)pyridine iron alkyl complexes have been long-sought-after targets due to the likely intermediacy of such species in olefin polymerization catalysis. Here we establish that bis(imino)pyridine iron monoalkyl complexes having three formal oxidation states (cation, neutral, and anion) all contain ferrous centers, and the redox chemistry is confined to the chelate. For neopentyl and neosilyl derivatives, the neutral and monoanionic forms of the bis(imino)pyridine are sufficiently weak field that high spin ferrous compounds result. In the case of the anion, the field strength increases sufficiently that a low

spin, d^6 compound results and dinitrogen coordination results. These studies imply that the ferrous oxidation state is maintained during treatment of (^{iPr}PDI)FeCl$_2$ with MAO and that redox events are confined to the bis(imino)pyridine chelate.

Experimental Section

General Considerations. All air- and moisture-sensitive manipulations were carried out using standard vacuum line, Schlenk, and cannula techniques or in an MBraun inert atmosphere drybox containing an atmosphere of purified nitrogen. Solvents for air- and moisture-sensitive manipulations were initially dried and deoxygenated using literature procedures.[60] Hydrogen and deuterium gas were passed through a column containing manganese oxide supported on vermiculite and 4 Å molecular sieves before admission to the high-vacuum line. Benzene-d_6 and toluene-d_8 were purchased from Cambridge Isotope Laboratories and dried over 4 Å molecular sieves or titanocene, respectively. (^{iPr}PDI)Fe(CH$_2$SiMe$_3$),[36] (^{iPr}PDI)-Fe(CH$_2$CMe$_3$),[36] (^{iPr}PDI)FeCH$_3$,[33] [(^{iPr}PDI)Fe(CH$_2$SiMe$_3$)(Et$_2$O)]-[BPh$_4$],[40] [(^{iPr}PDI)Fe(CH$_2$SiMe$_3$)(THF)][BPh$_4$],[40] [(^{iPr}PDI)Fe(CH$_2$-SiMe$_2$CH$_2$SiMe$_3$)][MeB(C$_6$F$_5$)$_3$],[40] and [Li(Et$_2$O)$_3$][(^{iPr}PDI)Fe(C$_6$H$_4$-4-R)(N$_2$)][35] were prepared according to literature procedures.

^{1}H NMR spectra were recorded on Varian Mercury 300 and Inova 400 and 500 spectrometers operating at 299.76, 399.78, and 500.62 MHz, respectively. All ^{1}H NMR chemical shifts are reported relative to SiMe$_4$, using ^{1}H (residual) chemical shifts of the solvent as a secondary standard. Peak width at half-height is given for paramagnetically broadened resonances. Elemental analyses were performed at Robertson Microlit Laboratories, Inc., Madison, NJ.

Solution magnetic moments were determined by the method[61] of Evans using a ferrocene standard and are the average value of at least two independent measurements. Solid state magnetic susceptibility measurements were performed with a Johnson Matthey magnetic susceptibility balance (MSB) that was calibrated with HgCo(SCN)$_4$ or using SQUID magnetometry. SQUID magnetization data of crystalline powdered samples were recorded with a SQUID magnetometer (Quantum Design) at 10 kOe between 5 and 300 K for all samples. Values of the magnetic susceptibility were corrected for the underlying diamagnetic increment by using tabulated Pascal constants and the effect of the blank sample holders (gelatin capsule/straw). Samples used for magnetization measurement were recrystallized multiple times and checked for chemical composition by ^{1}H NMR spectroscopy. The program julX, written by E. Bill, was used for (elements of) the simulation and analysis of magnetic susceptibility data.[62]

Single crystals suitable for X-ray diffraction were coated with polyisobutylene oil in a drybox, transferred to a nylon loop, and then quickly transferred to the goniometer head of a Bruker X8 APEX2 diffractometer equipped with a molybdenum X-ray tube (λ = 0.71073 Å). Preliminary data revealed the crystal system. A

(60) Pangborn, A. B.; Giardello, M. A.; Grubbs, R. H.; Rosen, R. K.; Timmers, F. J. *Organometallics* **1996**, *15*, 1518.
(61) Sur, S. K. *J. Magn. Reson.* **1989**, *82*, 169.
(62) http://ewww.mpi-muelheim.mpg.de/bac/logins/bill/julX_en.php.

hemisphere routine was used for data collection and determination of lattice constants. The space group was identified and the data were processed using the Bruker SAINT+ program and corrected for absorption using SADABS. The structures were solved using direct methods (SHELXS), completed by subsequent Fourier synthesis, and refined by full-matrix least-squares procedures.

Quantum-Chemical Calculations. All DFT calculations were performed with the ORCA program package.[63] The geometry optimizations of the complexes and single-point calculations on the optimized geometries were carried out at the B3LYP level[64−66] of DFT. This hybrid functional often gives better results for transition metal compounds than pure gradient-corrected functionals, especially with regard to metal−ligand covalency.[67] The all-electron Gaussian basis sets were those developed by the Ahlrichs group.[68,69] Triple-ζ-quality basis sets TZVP with one set of polarization functions on the metal and on the atoms directly coordinated to the metal center were used.[69] For the carbon and hydrogen atoms, slightly smaller polarized split-valence SV(P) basis sets were used that were of double-ζ quality in the valence region and contained a polarizing set of d-functions on the non-hydrogen atoms.[68] Auxiliary basis sets used to expand the electron density in the resolution-of-the-identity (RI) approach were chosen[70−72] to match the orbital basis.

The SCF calculations were tightly converged (1×10^{-8} E$_h$ in energy, 1×10^{-7} E$_h$ in the density change, and 1×10^{-7} in maximum element of the DIIS error vector). The geometry optimizations for all complexes were carried out in redundant internal coordinates without imposing symmetry constraints. In all cases, the geometries were considered converged after the energy change was less than 5×10^{-6} E$_h$, the gradient norm and maximum gradient element were smaller than 1×10^{-4} and 3×10^{-4} E$_h$ bohr^{-1}, respectively, and the root-mean-square and maximum displacements of all atoms were smaller than 2×10^{-3} and 4×10^{-3} bohr, respectively.

Throughout this paper we describe our computational results by using the broken-symmetry (BS) approach described by Ginsberg[73] and Noodleman.[74] Because several BS solutions to the spin-unrestricted Kohn−Sham equations may be obtained, the general notation BS(m,n)[75] has been adopted, where m (n) denotes the number of spin-up (spin-down) electrons at the two interacting fragments. Canonical and corresponding[76] orbitals as well as spin density plots were generated with the program Molekel.[77] Non-relativistic single-point calculations on the optimized geometries were carried out to predict Mössbauer spectral parameters (isomer shifts and quadrupole splittings). These calculations employed the

CP(PPP) basis set[78] for iron. The Mössbauer isomer shifts were calculated from the computed electron densities at the iron centers as previously described.[79]

Preparation of [Li(Et$_2$O)$_3$][(^{iPr}PDI)Fe(CH$_2$CMe$_3$)N$_2$]. A 50 mL round-bottom flask was charged with 0.150 g (0.25 mmol) of (^{iPr}PDI)Fe(N$_2$)$_2$ and approximately 20 mL of diethyl ether. The contents of the flask were cooled to −35 °C. A scintillation vial was charged with 0.020 g (0.25 mmol) of neopentyl lithium and approximately 10 mL of diethyl ether, and the resulting solution was cooled to −35 °C. The flask containing the iron compound was stirred, and the neopentyl lithium solution was added dropwise over the course of 5 min. The reaction was warmed to room temperature and stirred. After 0.5 h, the reaction mixture was filtered through Celite. The filtrate was collected, and the volatiles were removed. The resulting residue was dissolved in a minimal amount of diethyl ether, and the resulting solution was placed in a scintillation vial and cooled overnight at −35 °C for recrystallization. The resulting solid was collected on a glass frit and yielded 0.078 g (34%) of [Li(Et$_2$O)$_3$][(^{iPr}PDI)Fe(CH$_2$CMe$_3$)(N$_2$)]. Analysis for C$_{50}$H$_{84}$N$_5$FeO$_3$Li, calcd: C, 69.34; H, 9.78; N, 8.09. Found: C, 69.73; H, 8.92; N, 8.84. Magnetic susceptibility (benzene-d_6, 23 °C): $\mu_{eff} = 0$ μ_B. IR (KBr): ν(N$_2$) = 1948 cm^{-1}.

Alternative Preparation of [Li(Et$_2$O)$_3$][(^{iPr}PDI)Fe(CH$_2$CMe$_3$)-(N$_2$)]. This molecule was prepared using a procedure identical to that described above, with the exception that 0.100 g (0.14 mmol) of (^{iPr}PDI)FeBr and 0.022 g (0.28 mmol) of neopentyl lithium were used as the reagents. Recrystallization from diethyl ether at −35 °C furnished 0.052 g (41%) of [Li(Et$_2$O)$_3$][(^{iPr}PDI)Fe-(CH$_2$CMe$_3$)(N$_2$)].

Preparation of [Li(12-Crown-4)][(^{iPr}PDI)Fe(CH$_2$CMe$_3$)(N$_2$)]. A scintillation vial was charged with 0.05 g (0.06 mmol) of [Li(Et$_2$O)$_3$][(^{iPr}PDI)Fe(CH$_2$SiMe$_3$)(N$_2$)] and approximately 5 mL of diethyl ether. A solution containing 0.02 g (0.12 mmol) of 12-crown-4 in diethyl ether was added to the stirring solution of iron compound. The volume of the solution was reduced to approximately 5 mL, and the vial was placed in a −35 °C freezer. The solvent was decanted, and the solid was dried under reduced pressure to yield 0.030 g (64%) of a dark red-brown solid, identified as [Li(12-Crown-4)][(^{iPr}PDI)Fe(CH$_2$CMe$_3$)(N$_2$)]. Analysis for C$_{46}$H$_{70}$N$_5$FeO$_4$Li, calcd: C, 67.39; H, 8.61; N, 8.54. Found: C, 67.06; H, 8.42; N, 8.34. Magnetic susceptibility: $\mu_{eff} = 0$ μ_B. IR (KBr): ν(N$_2$) = 1996 cm^{-1}.

Attempted Preparation of [Li(Et$_2$O)$_3$][(^{iPr}PDI)Fe(CH$_2$SiMe$_3$)-(N$_2$)]. Attempts to synthesize this compound were carried out using the methods described above to successfully prepare [Li(Et$_2$O)$_3$][(^{iPr}PDI)Fe(CH$_2$CMe$_3$)(N$_2$)]. In a typical experiment, 0.300 g (0.50 mmol) of (^{iPr}PDI)Fe(N$_2$)$_2$ and 0.047 g (0.53 mmol) of LiCH$_2$SiMe$_3$ were used. Recrystallization from diethyl ether at −35 °C furnished 0.24 g (51%) of red crystals, identified as (^{iPr}PDI)Fe(CH$_2$SiMe$_3$), containing about 5% (as judged by Mössbauer spectroscopy) of the desired [Li(Et$_2$O)$_3$][(^{iPr}PDI)Fe-(CH$_2$SiMe$_3$)(N$_2$)]. IR (KBr): ν(N$_2$) = 1938 cm^{-1}.

Preparation of [(^{iPr}PDI)Fe(CH$_2$CMe$_3$)][BPh$_4$]. A 20 mL scintillation vial was charged with 0.100 g (0.164 mmol) of (^{iPr}PDI)Fe(CH$_2$CMe$_3$), 0.083 g (0.164 mmol) of [Cp$_2$Fe][BPh$_4$], and a stir bar. Approximately 7 mL of benzene was added to the mixture of solids with stirring. The stirring rate was increased as the reaction mixture thickened and a precipitate formed. After 5 min, an equal volume of pentane was added, and the stirring was continued for another 10 min. The solid was collected on a glass frit and washed four times with ~20 mL of pentane. The solid was dried under vacuum and yielded 0.143 g (93%) of a dull gray-red powder, identified as [(^{iPr}PDI)Fe(CH$_2$CMe$_3$)][BPh$_4$]. Analysis for C$_{62}$H$_{74}$N$_3$FeB, calcd: C, 80.25; H, 8.04; N, 4.53. Found: C, 80.41; H, 7.84; N, 4.21. Magnetic susceptibility (MSB, 23 °C): $\mu_{eff} = 4.8$

(63) Neese, F. *Orca—an ab initio, DFT and Semiempirical Electronic Structure Package*, Version 2.7, Revision 0; Institut für Physikalische und Theoretische Chemie, Universität Bonn: Bonn, Germany, August 2009.

(64) Becke, A. D. *J. Chem. Phys.* **1986**, *84*, 4524.

(65) Becke, A. D. *J. Chem. Phys.* **1993**, *98*, 5648.

(66) Lee, C. T.; Yang, W. T.; Parr, R. G. *Phys. Rev. B* **1988**, *37*, 785.

(67) Neese, F. Solomon, E. I. In *Magnetism: From Molecules to Materials*; Miller, J. S., Drillon, M., Eds.; Wiley: New York, 2002; Vol. 4, p 345.

(68) Schäfer, A.; Horn, H.; Ahlrichs, R. *J. Chem. Phys.* **1992**, *97*, 2571.

(69) Schäfer, A.; Huber, C.; Ahlrichs, R. *J. Chem. Phys.* **1994**, *100*, 5829.

(70) Eichkorn, K.; Weigend, F.; Treutler, O.; Ahlrichs, R. *Theor. Chem. Acc.* **1997**, *97*, 119.

(71) Eichkorn, K.; Treutler, O.; Öhm, H.; Häser, M.; Ahlrichs, R. *Chem. Phys. Lett.* **1995**, *240*, 283.

(72) Eichkorn, K.; Treutler, O.; Öhm, H.; Häser, M.; Ahlrichs, R. *Chem. Phys. Lett.* **1995**, *242*, 652.

(73) Ginsberg, A. P. *J. Am. Chem. Soc.* **1980**, *102*, 111.

(74) Noodleman, L.; Peng, C. Y.; Case, D. A.; Mouesca, J. M. *Coord. Chem. Rev.* **1995**, *144*, 199.

(75) Kirchner, B.; Wennmohs, F.; Ye, S.; Neese, F. *Curr. Opin. Chem. Biol.* **2007**, *11*, 134.

(76) Neese, F. *J. Phys. Chem. Solids* **2004**, *65*, 781.

(77) *Molekel*, Advanced Interactive 3D-Graphics for Molecular Sciences; available under http://www.cscs.ch/molkel/.

(78) Neese, F. *Inorg. Chim. Acta* **2002**, *337*, 181.

(79) Sinnecker, S.; Slep, L. D.; Bill, E.; Neese, F. *Inorg. Chem.* **2005**, *44*, 2245.

μ_B. ^{1}H NMR (benzene-d_6): δ −124.31 (569 Hz, 2H), −43.32 (470 Hz, 12H), −17.35 (258 Hz, 12H,), −0.70 (316 Hz, 4H), 4.61 (64 Hz, 4H), 12.33 (101 Hz, 8H), 23.25 (64 Hz, 8H), 101.95 (1042 Hz, 6H). ^{1}H NMR (fluorobenzene-d_5): δ −132.53 (588 Hz, 2H), −44.57 (237 Hz, 12H), −17.84 (116 Hz, 12H,), −0.01 (115 Hz, 4H), 5.89 (158 Hz, 4H), 10.60 (158 Hz, 8H), 28.98 (98 Hz, 8H), 73.41 (1138 Hz, 2H), 106.58 (528 Hz, 6H), 133.40 (611 Hz, 1H).

Preparation of [(^{iPr}PDI)Fe(CH$_2$CMe$_3$)(THF)][BPh$_4$]. A 20 mL scintillation vial was charged with 0.050 g (0.054 mmol) of [(^{iPr}PDI)Fe(CH$_2$CMe$_3$)][BPh$_4$]. A minimum amount of THF was added to dissolve the solid, forming a blue solution. The blue solution was layered with approximately 1.5 mL of pentane, and the vial was placed in a −35 °C freezer. Over the course of 8 h, a blue solid formed. The mother liquor was decanted, and the solid was dried at room temperature under vacuum, yielding 0.045 g (84%) of a light blue solid, identified as [(^{iPr}PDI)Fe(CH$_2$CMe$_3$)(THF)][BPh$_4$]. Analysis for C$_{66}$H$_{82}$N$_3$OFeB, calcd: C, 79.27; H, 8.26; N, 4.20. Found: C, 78.78; H, 7.96; N, 3.94. Magnetic susceptibility (MSB, 23 °C): μ_{eff} = 4.9 μ_B.

Preparation of [(^{iPr}PDI)Fe(CH$_2$CMe$_3$)(OEt$_2$)][BPh$_4$]. This compound was prepared in a manner similar to that used for [(^{iPr}PDI)Fe(CH$_2$CMe$_3$)(THF)][BPh$_4$] by dissolving 0.050 g (0.054 mmol) of [(^{iPr}PDI)Fe(CH$_2$CMe$_3$)][BPh$_4$] in approximately 5 mL of diethyl ether. Recrystallization from diethyl ether at −35 °C furnished 0.045 g (84%) of a light blue solid, identified as [(^{iPr}PDI)Fe(CH$_2$CMe$_3$)(OEt$_2$)][BPh$_4$]. Analysis for C$_{66}$H$_{84}$N$_3$OFeB, calcd: C, 79.11; H, 8.45; N, 4.19. Found: C, 78.78; H, 7.96; N, 3.94. Magnetic susceptibility (MSB, 23 °C): μ_{eff} = 4.8 μ_B.

Alternative Preparation of [(^{iPr}PDI)Fe(CH$_2$SiMe$_3$)][BPh$_4$]. This molecule was prepared in a manner similar to that used for [(^{iPr}PDI)Fe(CH$_2$CMe$_3$)][BPh$_4$] with 0.150 g (0.240 mmol) of (^{iPr}PDI)Fe(CH$_2$SiMe$_3$) and 0.121 g (0.240 mmol) of [Cp$_2$Fe][BPh$_4$] and yielded 0.199 g (88%) of a dull gray-red powder, identified as [(^{iPr}PDI)Fe(CH$_2$SiMe$_3$)][BPh$_4$] as reported previously.[40]

Alternative Preparation of [(^{iPr}PDI)Fe(CH$_2$SiMe$_3$)(THF)]-[BPh$_4$]. This molecule was prepared in a manner similar to that used for [(^{iPr}PDI)Fe(CH$_2$CMe$_3$)(THF)][BPh$_4$] with 0.050 g (0.240 mmol) of [(^{iPr}PDI)Fe(CH$_2$SiMe$_3$)][BPh$_4$] and yielded 0.049 g (96%) of a light blue powder, identified as [(^{iPr}PDI)Fe(CH$_2$SiMe$_3$)-(THF)][BPh$_4$] as reported previously.[40]

Alternative Preparation of [(^{iPr}PDI)Fe(CH$_2$SiMe$_3$)(OEt$_2$)]-[BPh$_4$]. This molecule was prepared in a manner similar to that used for [(^{iPr}PDI)Fe(CH$_2$CMe$_3$)(OEt$_2$)][BPh$_4$] with 0.050 g (0.240

mmol) of [(^{iPr}PDI)Fe(CH$_2$SiMe$_3$)][BPh$_4$]. The addition of ether resulted in an immediate color change of the solid to blue and yielded 0.050 g (98%) of a light blue powder, identified as [(^{iPr}PDI)Fe(CH$_2$SiMe$_3$)(OEt$_2$)][BPh$_4$] as reported previously.[40]

Preparation of [(^{iPr}PDI)FeCH$_3$][BPh$_4$]. This molecule was prepared in a manner similar to that used for [(^{iPr}PDI)Fe-(CH$_2$CMe$_3$)][BPh$_4$], but with 0.112 g (0.202 mmol) of (^{iPr}PDI)-FeCH$_3$ and 0.100 g (0.200 mmol) of [Cp$_2$Fe][BPh$_4$]. The light red solid was collected on a glass frit and washed four times with ∼20 mL of pentane. The solid was dried under vacuum and yielded 0.153 g (89%) of a dull gray-red powder, identified as [(^{iPr}PDI)FeCH$_3$][BPh$_4$]. Single crystals suitable for X-ray diffraction were grown by dissolving 0.020 g (0.036 mmol) of (^{iPr}PDI)FeCH$_3$ in 1 mL of C$_6$H$_5$F and adding 0.016 g (0.032 mmol) of [Cp$_2$Fe][BPh$_4$]. After being stirred for 1 min with a glass pipet, the resulting solution was filtered through a glass frit into an NMR tube and layered with *n*-hexane. The layers were allowed to diffuse together over the course of 36 h at room temperature, yielding translucent blocks with a reddish-brown hue. Analysis for C$_{58}$H$_{66}$N$_3$FeB, calcd: C, 79.90; H, 7.63; N, 4.82. Found: C, 79.62; H, 7.86; N, 4.57. Magnetic susceptibility (MSB, 23 °C): μ_{eff} = 5.2 μ_B. ^{1}H NMR (benzene-d_6): δ −115.45 (1715 Hz), −49.31 (1665 Hz), −17.53 (216 Hz), −8.15 (380 Hz), 1.95 (102 Hz), 8.40 (114 Hz), 9.31 (455 Hz), 20.40 (102 Hz), 81.49 (1850 Hz), 131.31 (1053 Hz). ^{1}H NMR (fluorobenzene-d_5): δ −117.93 (985 Hz, 2H), −46.66 (873 Hz, 12H), −18.36 (454 Hz, 12H), −0.71 (284 Hz, 4H), 3.73 (186 Hz, 4H), 8.73 (198 Hz, 8H), 12.21 (221 Hz, 8H), 68.61 (730 Hz, 2H), 185.38 (855 Hz, 6H), 128.03 (513 Hz, 1H).

Supporting Information Available: Crystallographic details for [(^{iPr}PDI)Fe(CH$_2$CMe$_3$)][BPh$_4$], [(^{iPr}PDI)FeMe][BPh$_4$], and [Li(Et$_2$O)$_3$][(^{iPr}PDI)Fe(CH$_2$CMe$_3$)(N$_2$)] in CIF format. This material is available free of charge via the Internet at http://pubs.acs.org.

JA106575B